SONY
make.believe

Master of Science Thesis

Co-located Antenna Design in a Mobile Phone

By

Russ Whiton and Farzaneh Firouzabadi

Department of Electrical and Information Technology
Faculty of Engineering, LTH, Lund University
SE-221 00 Lund, Sweden

Master's Thesis Report – Co-located Antenna Design in a Mobile Phone

Lund Tekniska Högskola (LTH) – Lund, Sweden

Russ Whiton – russjwhiton@gmail.com

Farzaneh Firouzabadi – f.firouzabadi@gmail.com

LTH Supervisor: Buon Kiong Lau – buon_kiong.lau@eit.lth.se

In conjunction with **Sony Mobile Communications (SMC)**

SMC Adviser: Scott Vance – scott.vance@sonymobile.com

SMC Manager: Mikael Persson – mikael.m.persson@sonymobile.com

Abstract

Smartphones integrate a large number of wireless technologies into one handheld device. Designing antennas for these devices is more challenging than ever with an increasing number of technologies and frequency bands compacted into smaller and smaller packages. Many devices need four or more antennas to integrate all the technologies demanded of competitive products.

Multiple-Input-Multiple-Output (MIMO) antenna systems have added a new level of complexity for antenna designers. In particular, to realize the gains MIMO offers for the two-antenna case, both antennas on the phone need to operate simultaneously on the same frequencies. Moreover, these antennas should not only be isolated from the power transmitted or received by each other, but their signals should also be uncorrelated.

The design choice of where along the top, bottom, or sides of the phone to place the antenna is an important one. Perhaps the biggest challenge is placing the two antennas such that they meet the isolation and correlation requirements for MIMO applications. If the two could be placed side-by-side at one end of the phone it would allow for increased design flexibility. Greater design flexibility is extremely important with real-estate on the circuit board becoming a critical limitation as more features are packed into smaller spaces.

This project explores in detail two new proposals for co-locating the antennas at the bottom of a handset and compares the results to previous work. This report discusses advantages and disadvantages of each method along with an analysis of key performance parameters.

Acknowledgments

We owe a great deal of thanks to our Sony advisor, Scott Vance, for sharing his extensive experience with us and being a pleasure to deal with on a personal level.

We were also very fortunate to have our LTH adviser, (Vincent) Buon Kiong Lau, whose round-the-clock willingness to help led us to speculate that he never sleeps. It is an honor to work under someone so accomplished and respected in the field of MIMO communications.

Our manager, Mikael Persson, demonstrated how a manager should operate. By coordinating resources to ensure we had the tools we needed to get the job done, our success would be a function of our own work ethic and abilities, and not limited by resource constraints.

Johan Andersson and his CST expertise were extremely valuable. Rune Sø, Gordon Brown, Kenneth Håkansson, and the rest of the antenna product development group were always more than willing to take time out of their schedules to answer our questions and share their years of experience.

Walther Borg, Max Kruse, and Katarina Lundquist were always quick to fix any resource problems or administrative problems.

Thanks are owed to Zhinong Ying, Mikael Håkansson, and all of the thesis workers before us who laid the groundwork for the project.

Special thanks to Peter, Helena, and Elliot Jones for being such great friends and making Sweden feel like home.

Russ Whiton and Farzaneh Firouzabadi

Table of Contents

Preface

In recent years, Sony has sponsored several thesis projects that have attempted to push the boundaries of antenna placement in a mobile phone, particularly looking forward to MIMO designs.

Numerous challenges present themselves when an attempt is made to create a MIMO antenna system that is functional at low frequencies, especially given the size constraints on the scale of a mobile phone.

Among others, Mikael Håkansson explored this topic in his thesis "Decoupling Techniques for a Multiband MIMO Antenna System". Using both single-band and dual-band monopoles, he explored a number of different techniques for improving both isolation and correlation with narrowly spaced antennas, including neutralization lines, hybrid couplers, and lumped elements.

To address multi-band requirements in a compact phone size, Kin-Lu Wong and Cheng-Tse Lee at National Sun Yat-Sen University in Taiwan created a multi-band single-antenna intended for mobile phones with a thin profile, and shared the results in the journal *Microwave and Optical Technology Letters*.

In addition, Sony Mobile Communications has created an antenna concept with multiple resonances in a small geometry to develop a "co-located" configuration with two antennas on one end of the phone. The resulting configuration is an excellent proof of concept, which can be used as a reference to study alternate configurations of the same concept as well as those of other antenna concepts.

Accordingly, Sony's product development antenna engineers have created a variety of antenna concepts that are robust and promising enough to be modified and refined into working MIMO antenna systems.

This thesis builds on the hard work and results produced by all of these parties. Two primary cellular antenna design concepts from Sony were taken and studied extensively. After gaining an understanding of critical parameters and the theory behind the operation of each antenna, they were

modified in a two-step process to create a co-located MIMO antenna system.

The first step was to reduce the physical size of the antennas without making significant sacrifices in the performance. Both of the original antennas occupy almost the same whole bottom region of the phone. A co-located design requires that each antenna element occupies an absolute maximum of half of the phone width.

The next step was mirroring or duplicating the designs in some fashion to create a two-antenna system. Numerous complications arose when the second antenna was introduced, and a number of methods were explored to address or at least understand these issues.

Despite using the two-step process as a general guideline, the antenna design work was largely based on trial and error that involved many experiments and iterations. However, the results are presented in a more linear fashion for the sake of ease of reading.

Russ Whiton was responsible for the inductively fed (L-Fed) design, and Farzaneh Firouzabadi was responsible for the capacitively fed (C-Fed) design. The work on each antenna was done independently, but the analysis of the reference design, processing of results, writing of the report, and solving of all other project challenges were equally shared.

The goal was to modify both designs to produce a MIMO antenna system that is compliant with the mobile operator performance specifications detailed in Chapter 1 in a package small enough that it could be integrated into a mobile phone.

CHAPTER 1

1 Introduction

1.1 Background

Phone manufacturers have a keen interest in exploring any technique that can save space in a handset. Integrated circuits have more and more functionality built into smaller packages, discrete components are shrinking to microscopic sizes, and board layouts are astoundingly tight. Early-stage board designs hold room for an aggressively small number of component placeholders to reduce the time between early prototypes and final products. Therefore, space-saving measures are essential for compacting the overall design.

A challenge separates wireless devices from conventional electronics—one of the most fundamental requirements for allowing antennas to resonate is having sufficient physical space and separation from the phone. The first few generations of mobile phones relied on a simple "rubber duck" whip antenna extending from the phone, often as long as the phone itself. This evolved into smaller versions like the stubby antenna, and now it is virtually impossible to find a mobile phone that does not use an internal antenna. Figure 1 illustrates the evolution of mobile antenna designs.

Antenna design is one of the many areas of mobile phone design where the performance requirements are becoming more demanding while the allotted space shrinks. To meet these requirements, an antenna engineer must find a clever way to utilize every cubic millimeter of space given to him or her.

Making things even more challenging, in addition to operating on various cellular standards (GSM, CDMA2000, WCDMA, HSPA+, LTE), modern smartphones must include Bluetooth, Wireless LAN and GPS as well.

Figure 1. (Left) Motorola DynaTAC with whip antenna **[1]** (Middle) LG VX8300 with stubby antenna **[2]** (Right) Sony Ericsson Xperia with internal microstrip antenna **[3]**

Many third-generation cellular receiver chipsets on the market allow for receive diversity, that is, the ability to combine information from two separate receive antennas. Adding the second cellular antenna allows for considerable gains in throughput; these gains are significant enough that many wireless carriers are mandating that yet another antenna be added to this end.

The most difficult antenna to design is certainly the cellular antenna. It will have the largest fractional bandwidth and must have multiple resonances to cover different frequency bands. Different countries have their own unique spectrum allocations, and as a result, there are dozens of frequency bands for each cellular protocol depending on the region of the world where the phone is intended to operate.

Fourth-generation cellular protocols are beginning to utilize the idea of Multiple-Input-Multiple-Output (MIMO) communication. In a MIMO system, both the transmitter and receiver may have more than one antenna that can send and receive information independently (discussed in more detail in the following sections), and as a result, each antenna needs to have strong performance individually and be isolated from one another.

An extremely large number of configurations are possible by placing the antennas at different locations along the top, bottom, and sides of the phones. However, one limitation encountered in existing work is that the two cellular antennas cannot be placed next to each other in a "co-located" fashion and still satisfy the stringent parameter requirements necessary for MIMO. This thesis project explores whether that constraint can be lifted with several different new antenna concepts.

A successful co-located MIMO implementation will not only save precious space in the handset design, but it offers the possibility of another key advantage as well. Extensive studies have shown that the way a user holds a phone is critical to the performance; resonant frequencies and radiation patterns change dramatically as a result [4]. The transmit antennas may be switched dynamically to minimize the effect of body loss, resulting in better performing devices regardless of how the user holds the phone [5].

The remainder of this chapter provides the technical definitions necessary for understanding the report, along with the design target values. Tools used in both this project and the original reference designs are discussed in Chapter 2. The results of Sony's previous work used as a baseline are discussed in detail in Chapter 3. The two additional Sony antenna concepts that were modified are discussed in Chapters 4 and 5. Finally, a summary of the results is provided in Chapter 6, and conclusions are drawn in Chapter 7.

1.2 Terms and Definitions

Return Loss – Perhaps the most fundamental performance metric of an antenna, the return loss is a ratio of power reflected back to the power fed into the antenna. The frequencies where the return loss is high are called the resonant frequencies. It is most commonly expressed in decibel (dB).

Bandwidth – The range of frequencies surrounding a resonant frequency where the antenna resonates reasonably well. A high bandwidth antenna is resonant across a large range in frequency. It is typically expressed in MHz or as a percentage if the bandwidth is divided by the resonant frequency (i.e., fractional bandwidth). Common definitions define bandwidth of a resonant frequency as the range at which the return loss exceeds 3 or 6 dB.

Efficiency – A measure of the antenna losses, the efficiency is the ratio of power radiated to the power transmitted through the feed. Expressed as a percentage or more commonly in dB.

Gain – The magnitude of energy radiated outward from the antenna in a specific direction. It is typically expressed as a ratio (dBi) relative to the amount of energy radiated by a theoretical perfectly efficient antenna radiating energy uniformly in all directions. It refers to the peak of the pattern if given as a single value, but can also be given as a function of the polar coordinates of the full 3-D radiation pattern.

Isolation – In a multiple-antenna system, isolation gives the ratio of energy input into one antenna as a result of power being fed into another antenna. It is typically expressed in dB. Low isolation means a high percentage of energy output by one antenna (in the transmit mode) is being fed directly back into the system via another antenna, degrading system performance.

Correlation – In a multiple-antenna system, a quantification of the similarity of the radiation patterns of two antennas is the correlation. The correlation considers the polarization and gain as a function of frequency between the two antennas (see the next section for the more precise mathematical definition).

Specific Absorption Rate (SAR) – A measurement of the amount of radiation absorbed by the body when the phone is placed in specific orientations. Measured in Watts / Kg of body tissue.

Smith Chart – Perhaps the most informative and condensed display of information an antenna engineer can view. The Smith chart is a circular display of the complex response of an RF system normalized by the desired (or characteristic) impedance. The center of the chart represents a perfect match at a given frequency, and any deviation from this point shows the inductive or capacitive behavior of the mismatch as a function of frequency.

1.3 Performance Targets

1.3.1 Resonant Frequency and Bandwidth

Performance requirements are strictly set by several regulatory bodies. The most fundamental requirements are government regulatory bodies such as the United States' Federal Communications Commission (FCC) or Europe's European Telecommunications Standards Institute (ETSI). These government agencies regulate the power levels that wireless devices are allowed to transmit as a function of frequency in order to allow for a healthy wireless ecosystem with multiple technologies operating simultaneously across the electromagnetic spectrum. These requirements are usually met with relative ease.

Far more demanding are the requirements set by the main customers of handset vendors: the network operators. Network operators demand that devices meet sufficient performance requirements to ensure that end users have a satisfactory experience when using the network. An antenna design that fails to meet a certain level of efficiency and bandwidth will result in disgruntled customers visiting the carrier's retail locations asking for a fix or for replacement mobile phones.

The most fundamental design parameters of the antenna—the resonant frequencies and bandwidth—are decided by examining the most common frequency bands, which are listed in Table 1. These bands cover a significant portion of the largest target markets worldwide.

TABLE 1. FREQUENCY BANDS

System	Band	Uplink	Downlink
GSM-850	850	824.2-849.2	869.2–894.2
E-GSM-900	900	880.0–915.0	925.0–960.0
DCS-1800	1800	1710.2–1784.8	1805.2–1879.8
PCS-1900	1900	1850.2–1909.8	1930.2–1989.8
UMTS I	2100	1920-1980	2110-2170
LTE-17	700-Low	704-716	734-746
LTE-13	700-Mid	777-787	746-756
LTE-20	850 MHz EDD	832-862	791-821

Dozens of other band definitions overlap with these frequencies (e.g., the common CDMA2000 band classes BC0, BC1, BC15), but Table 1 lists the main non-overlapping target bands. Therefore, "lowband" is defined as a continuous block of frequencies from 704 MHz to 960 MHz unless otherwise specified. "Highband" refers to the continuous block of frequencies from 1710 MHz to 2170 MHz.

The LTE-7 Band includes frequencies in the 2500-2700 MHz range, but it is not targeted in this thesis and therefore omitted.

1.3.2 Efficiency and Gain

The specifications for parameters of gain and efficiency of the antenna are not individually specified by operators because operators are concerned primarily with system-level performance. Therefore, the same antenna paired with a poorly designed RF front-end may not necessarily pass all of the radiated performance tests. The two system-level tests where poor gain or efficiency becomes apparent are the Total Isotropic Sensitivity (TIS) and Total Radiated Power (TRP) tests.

TIS measures the average sensitivity around the full sphere by fixing the phone in a series of orientations throughout the 3-D space, where for each orientation the power is reduced until a certain packet or frame error rate is reached. TRP is a measure of the average value of power transmitted from the radio through the antenna around the full sphere.

Obviously, the gain and efficiency will largely determine the results of these two tests. By assuming a certain level of conducted performance from the radio it is possible to set goals for the efficiency and gain necessary to pass these tests with sufficient margin. The target values for efficiency as a function of frequency band are listed in Table 2.

TABLE 2. EFFICIENCY DESIGN TARGETS

Frequency Band	Free Space Efficiency (dB)
Lowband (704-960 MHz)	-3
Highband (1710-2170 MHz)	-4

1.3.3 Isolation

Isolation is important in a MIMO system. If the antennas are not sufficiently isolated, significant portion of the transmitted power will be directly fed into another antenna, degrading the efficiency. As a result, a problem with low isolation may show up in different test failures, including TIS/TRP failures.

At the base station, it is easy to get sufficient isolation between the antennas because the overall geometry can be multiples of a wavelength; therefore, the limiting factor for cellular systems for MIMO capacity gains is often isolation at the handset end (therefore, a function of handset size) [6].

1.3.4 Correlation

Antenna correlation is an important metric when designing a MIMO system. The correlation is a metric that quantifies the similarity between the radiation patterns of two given antennas. Equation (1) gives a closed form calculation for the envelope correlation coefficient ρ_e of antennas X and Y by using the radiation patterns (E) as a function of solid angle $\Omega = (\Phi, \theta)$

$$\rho_e = \frac{\left(\oint\left(XPRE_{\theta X}(\Omega)E^*_{\theta Y}(\Omega)P_{\theta}(\Omega)+E_{\Phi X}(\Omega)E^*_{\Phi Y}(\Omega)P_{\Phi}(\Omega)\right)d\Omega\right)^2}{\oint(XPRG_{\theta X}(\Omega)P_{\theta}(\Omega)+G_{\Phi X}(\Omega)P_{\Phi}(\Omega))d\Omega \oint(XPRG_{\theta Y}(\Omega)P_{\theta}(\Omega)+G_{\Phi Y}(\Omega)P_{\Phi}(\Omega))\, d\Omega} \quad (1)$$

XPR in this equation represents the Cross Polarization Ratio, the time average vertical power to the time average horizontal power [7] and *XPR* = 1 is assumed (i.e., full polarization mixing). *P* represents the angular power spectrum (either Φ or θ in polarization), and for the assumed isotropic incoming waves used to evaluate antenna correlation, it is given by $1/4\pi$. Moreover, *G* is defined by $|E|^2$ and * denotes the complex conjugate operator.

For MIMO systems to function well, the patterns should be very dissimilar either in their directions of orientation, their polarizations, or both. The less information that one pattern tells about the other, the more different the two resulting (spatial) channels look, and the easier the possibility to send information with unique spatial properties [8], [9].

1.3.5 Multiplexing Efficiency

Balancing the individual antenna efficiencies with the antenna correlation is a difficult task for the designer. Network operators have their own metric for envelope correlation and other performance tests determined by efficiency. However, a more generalized performance metric targeted at antenna engineers that expresses the impact of multi-antenna properties on MIMO system capacity in terms of equivalent loss in efficiency has been proposed, and it is called the Multiplexing Efficiency [10]. Equation (2) defines the Multiplexing Efficiency for the 2 × 2 MIMO case, which is of interest in this thesis (i.e., assuming ideal transmit antennas and antennas under test on the receive end).

$$\eta_{mux} = \sqrt{\eta_1 \eta_2 (1 - \rho_e)} \tag{2}$$

η_1, η_2 are the (total) efficiencies of antennas 1 and 2, respectively. The Multiplexing Efficiency allows the designer to directly understand the overall system performance tradeoff between antenna efficiency and correlation coefficient. When the envelope correlation coefficient ρ_e is above 0.5, the throughput loss becomes significant.

Wireless operators do not yet specify Multiplexing Efficiency, since the metric is a relatively recent development; therefore, there is no target specification. However, it is a useful tool for analyzing system performance.

CHAPTER 2

2 Simulation and Measurement Tools

2.1 CST Studio Suite

The CST Studio Suite is a package of software tools developed by Computer Simulation Technology AB [11]. The package includes software modules tailored to solve a variety of physics design problems. Among the modules are solvers specialized for electrostatics, thermal design, PCB Design, transmission line modeling, and others.

The primary module of interest in this project was the CST Microwave Studio. By making close approximations of Maxwell's equations, the high-frequency behavior of mechanical structures can be estimated.

The Finite-Difference Time-Domain (FD-TD) solver of CST Microwave Studio was utilized extensively. FD-TD solvers work by breaking a geometrical model into a three-dimensional grid (a Yee lattice) in small enough increments that the electromagnetic fields do not change significantly across adjacent increments (i.e., in the order of a small fraction of a wavelength) [12]. After setting the geometry into this fine grid, it is treated as an initial-value problem and an excitation is applied. Waves propagate outward from the source of the excitation and Maxwell's time-dependent curl equations are iteratively solved until a steady state condition is reached [13].

With the time-dependent curl equations solved, the user can look at the frequency response, phase response, electric and magnetic fields, current distributions, and far field radiation patterns.

Using CST Microwave Studio and breaking the geometry into a fine enough grid, very complicated and large problems may be solved with great accuracy. It is critical that a fine enough mesh be applied to small geometries or the results will be highly skewed. CST Microwave Studio allows the user to define localized grid spacing in different parts of the

model, and aspects of the model can be defined in terms of variables, making it easy to change the geometry quickly to save countless hours of tedious prototyping and measurement.

The other module utilized was the CST Design Studio. The CST Design Studio is a schematic design tool that works in tandem with the CST Microwave Studio by allowing the user to export the results as a schematic block. Matching circuits can be tested and optimized and the results combined. However, this tool is not as user-friendly or dynamic as the tool described in the following section and was therefore used only sparingly.

2.2 BetaMatch

BetaMatch is a software package developed and sold by a company specializing in antenna design tools and antenna design consulting: MNW Scan Pte Ltd [14].

BetaMatch allows the user to import return loss data for an unmatched RF circuit in the form of an .s1p file. After the user uploads the file, statistics are shown about the imported data including the intrinsic bandwidth and bandwidth potential. The user may then choose a matching topology and desired frequency bands, and the software will provide an ideal matching circuit.

An initial match may use ideal components, but another powerful feature of the program is the possibility of downloading dozens of libraries of measured data on components from manufacturers, giving even greater accuracy.

The graphical user interface allows for easy adjusting of components and visualization of how each component of the match will adjust the log magnitude response and Smith chart. Figure 2 shows a screen capture of the BetaMatch interface.

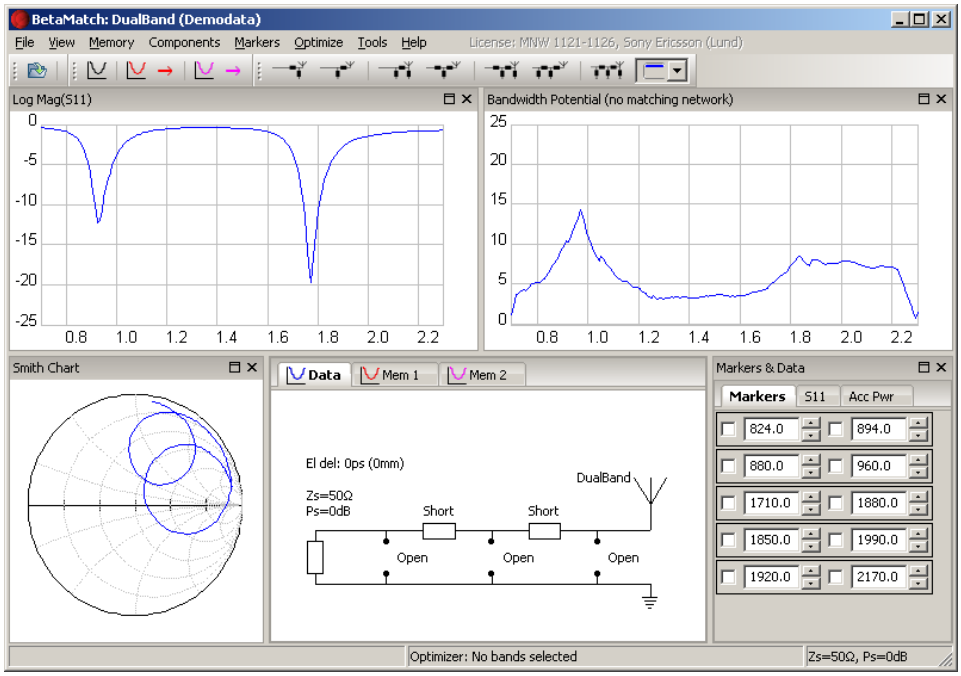

Figure 2. BetaMatch Interface

2.3 Mock-ups

Mock-ups are an essential tool in antenna design and verification. When the design is in its infancy, the easiest way to make quick changes is often to move pieces of copper tape and printed meander line around on a simple structure and view the changes on a network analyzer. This gives the first intuition of which parameters are critical for tuning the frequency response.

In this project, the original mock-ups were built by cutting a thin (typically one millimeter thick) sheet of plastic with a dielectric constant of approximately $\varepsilon_r \approx 2.6$ to approximate the ground plane size of a phone that is 60-70 mm in width and 120-130 mm in height.

Next, the boards were wrapped in copper tape. One end of the board was wrapped entirely in tape, and a 6-10 mm gap was left at the other corresponding to the antenna clearance from the ground plane. Finally, SMA antenna connectors were soldered along the side of the board to provide connections for the feed. One of these boards is shown in Figure 3.

Figure 3. Mock-up Board

A separate piece of plastic was used as a platform for printing the microstrip structure of the antenna, which was then taped and soldered to the board. The end result was a simple prototype that could go a long way towards approximating the antenna performance in a mobile phone. Figure 4 shows a more complete mock-up with matching and ground connections.

Modern antenna design is largely performed via simulation, and one of the most important features of a mock-up is the ability to verify those results. Errors and oversights in simulation can often give misleading results if meshing, excitations, boundary conditions, dielectric constant values, or geometry are not properly set up, and there is no substitute for having a piece of hardware to verify CAD results.

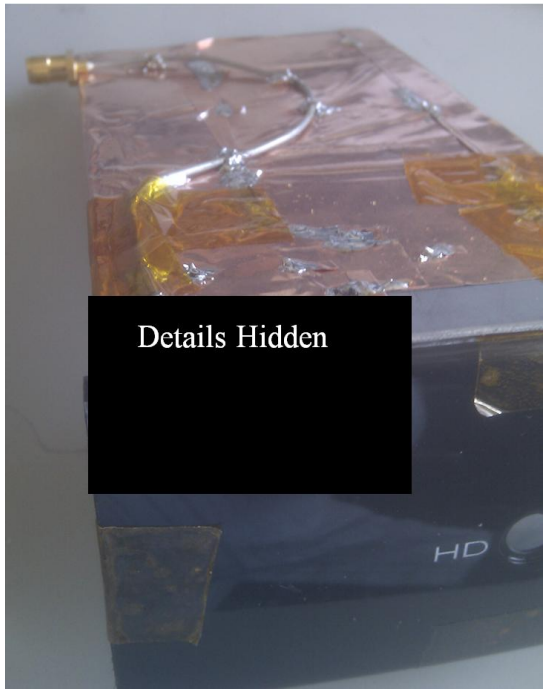

Figure 4. Completed Mock-up

2.4 Scattered Field Chambers

Testing the mock-ups requires a quiet RF environment without any interferers. Therefore, parameters such as efficiency and correlation were tested in scattered field chambers located in the Sony Mobile Communications antenna labs in Lund. The rooms are shielded from outside electromagnetic interference, and the cable losses are calibrated out and a series of predefined tests are established to measure key performance characteristics.

In mobile handset design, measuring efficiency typically requires integration of the radiation pattern over the entire sphere of the antenna to determine the power difference between the energy input to the antenna (the available energy) and the energy that is radiated [15]. However, this is not required for efficiency measurement in a scattered field chamber, which means it is a more efficient way to measure efficiency [16].

Figure 5 shows one of the shielded test rooms and the antenna mounting setup.

Figure 5. Scattered Field Chamber

The key performance parameters and merits of using the chamber were studied in detail in a previous Sony-sponsored thesis project [17].

CHAPTER 3

3 Reference Design

3.1 Project History

A small form-factor multiband antenna capable of covering the entirety of Table 1's frequency bands (and additional bands in the 2500-2600 MHz range) was created by Kin-Lu Wong and Cheng-Tse Lee at National Sun Yat-Sen University in Taiwan [18]. They created a printed two-strip monopole that can be folded into a small geometry extending from the end of the phone.

However, with a total length of 50 mm, it is not feasible to place two of these at the end of a phone.

Sony Mobile Communications has developed an antenna concept covering a similar range of frequencies but in a small enough volume that it may be used in a "Co-located" fashion. It provides a baseline for a MIMO LTE solution (with both antennas placed at the bottom of a phone) that is close to passing carrier specifications. Each antenna element needs to satisfy the bandwidth and efficiency targets while being sufficiently isolated and uncorrelated with the other. Furthermore, the design is intended to be viable for phones even with a slim form factor (less than 10-mm thickness).

There are a few limitations of the design in this form. One of the most important considerations is that the placement of a battery will significantly change the antenna efficiencies and radiation patterns, so any production model using the concept would need to address that considerable challenge.

Another possibility opened by successful implementation of the co-located antenna configuration was a four-element array (a set of the two-element configuration is placed on both the top and the bottom of the phone). Any combination of the two elements may be activated to negate hand and head effects [5].

This technology of dynamically adapting to the user's position is promising, but faces its own set of challenges in the practicalities of combining four cellular antennas with the other technologies, board real-estate, high linearity requirement on switching components, and front-end losses.

3.2 Theory

Figure 6 shows a conceptual picture of the reference design. The details have been simplified to illustrate the dimensions and concept.

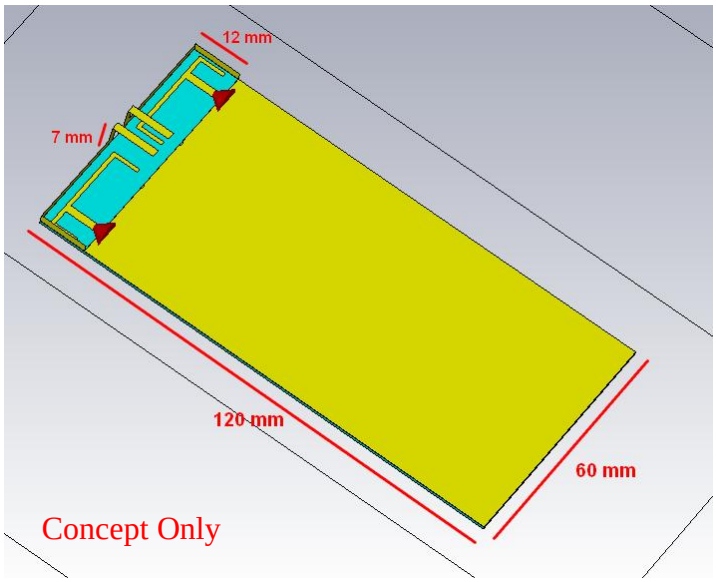

Figure 6. Reference Design Concept

The physical dimensions of the design are listed in Table 3. The final dimensions for the combined system are about twice those of a normal primary antenna, as expected. However, the geometry is significantly changed for each individual element.

The design covers most of the bands listed in Table 1, the most challenging of which are the 700 MHz LTE bands. It does not fully cover the 700-MHz band, as the results in the following section demonstrate. The inverse relationship between size and bandwidth is well established, but there are techniques that can be applied to artificially extend the bandwidth [19].

TABLE 3. REFERENCE DESIGN DIMENSIONS

Dimension	Size (mm)
Board Height	120
Board Width	60
Clearance (Upward from board)	12
Clearance (Out from board)	7

3.3 Performance

A CST simulation of one of the earlier reference design structures was utilized, along with a machined prototype. The results are compared in the following section.

3.3.1 Return Loss

The frequencies of Table 1 are covered with the exception of the sub-750 MHz frequencies, as shown below in Figure 7.

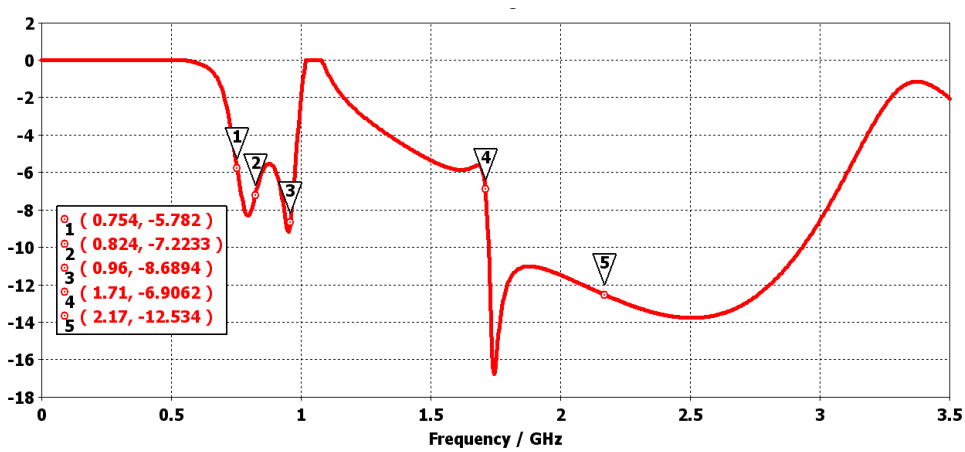

Figure 7. Reference Design Reflection Coefficient

Other than parasitic inductors, no discrete elements are used for matching. The Smith chart is shown in Figure 8. The measured return loss from the prototype is shown in Figure 9. The results are quite similar, though the simulation shows slightly better results.

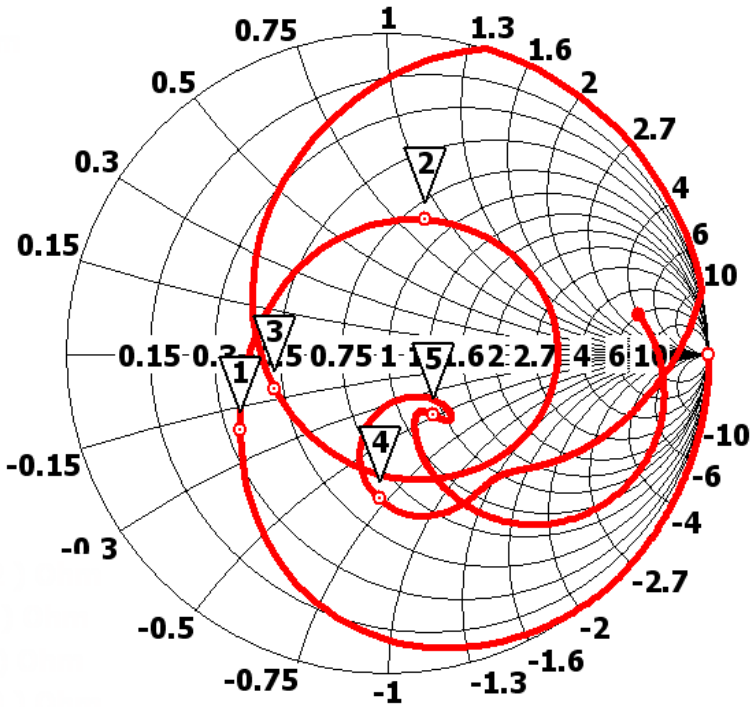

Figure 8. Reference Design Smith Chart

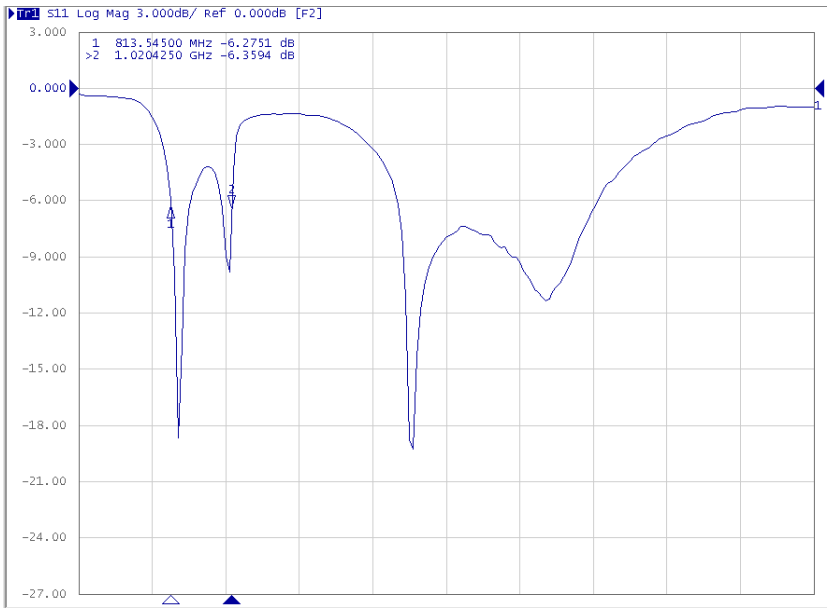

Figure 9. Reference Design Measured Reflection Coefficient

3.3.2 Isolation

The isolation is shown in Figure 10. The performance is extremely good in the highband, and reasonable in the lowband. At 791 MHz there is a peak value of around -7 dB. The measured antenna isolation is pictured in Figure 11, and good agreement with the simulated result is found.

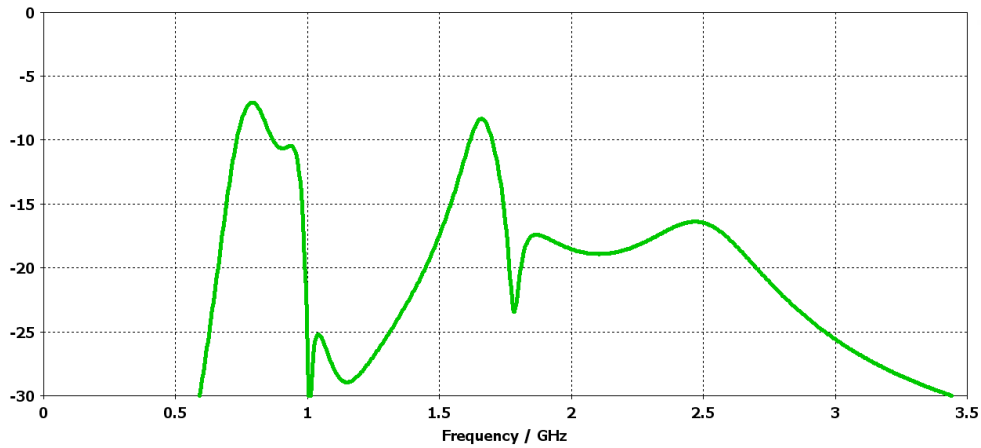

Figure 10. Reference Design Simulated Coupling Coefficient

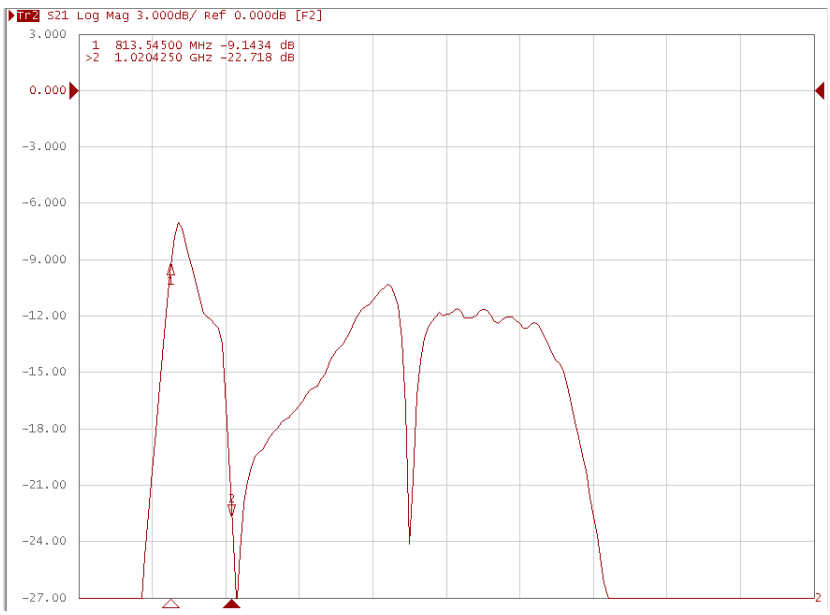

Figure 11. Reference Design Measured Coupling Coefficient

3.3.3 Efficiency

The simulated antenna efficiencies are quite good across both bands, dipping only slightly below the target -3 dB in the 700 MHz band, but the measured reference design fares a bit worse, especially at low frequency. The measured and simulated results are compared in Figure 12.

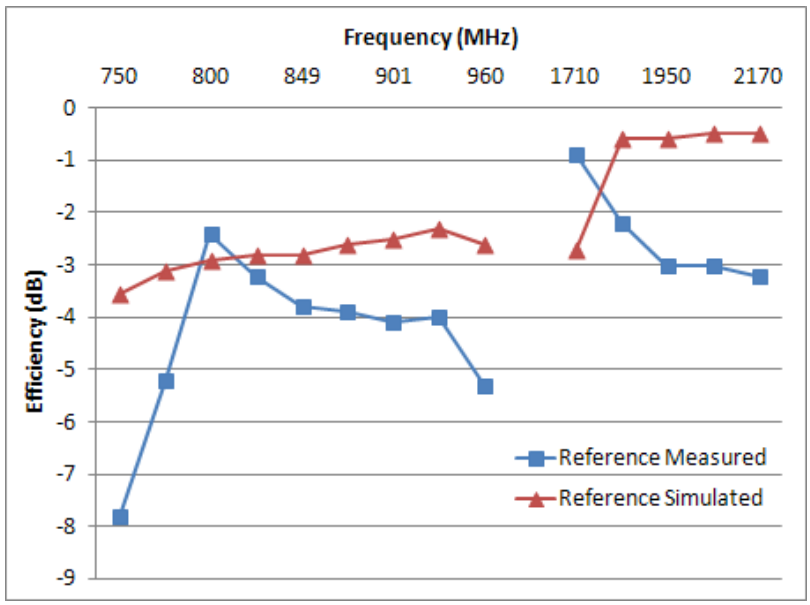

Figure 12. Reference Design Radiation Efficiency

3.3.4 Radiation Pattern

As with most phone designs, the correlation requirement is the most difficult aspect to pass at low frequencies. The lowband radiation pattern generated from exciting the right-hand port is shown in Figure 13 below. This pattern is far more omnidirectional than the high frequency pattern shown on the right of the figure.

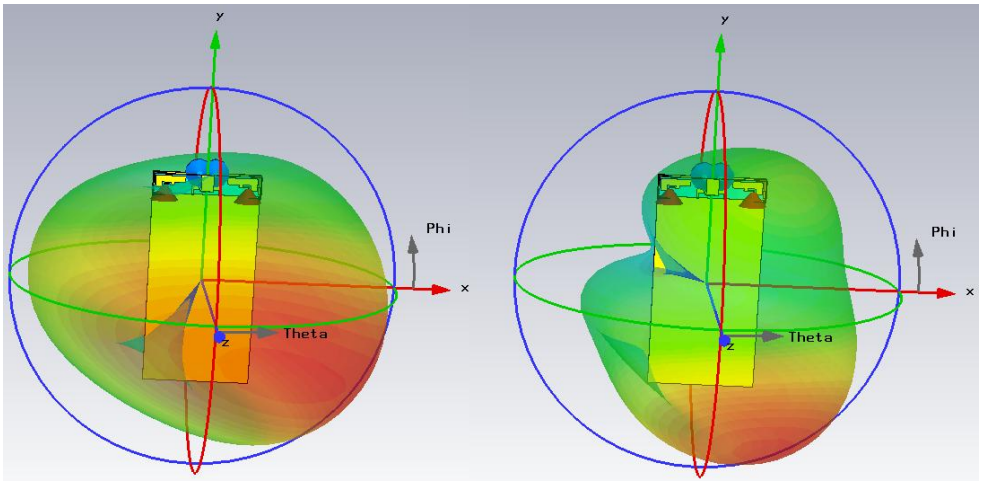

Figure 13. Reference Design Simulated Radiation Pattern 850 MHz (left) and 1950 MHz (right)

Figure 14 shows the measured radiation patterns. While the left maintains the omnidirectional pattern with the peak facing down and right, the highband maintains a similar shape as the simulation but is not as closely matched.

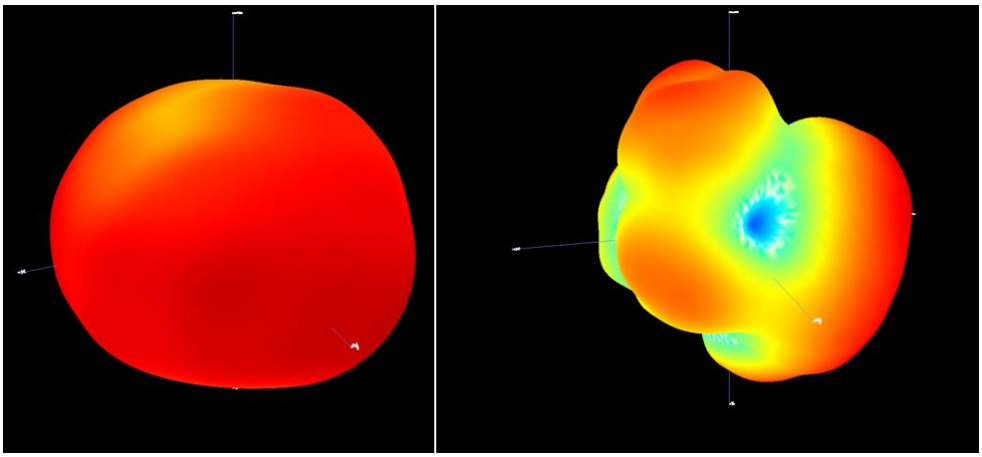

Figure 14. Reference Design Measured Radiation Pattern 850 MHz (left) and 1950 MHz (right)

3.3.5 Correlation

The correlation coefficient calculated from the far-fields of the simulated and measured design is shown in Figure 15. The values show a fairly consistent trend, with the first crossover frequency appearing at 800 MHz.

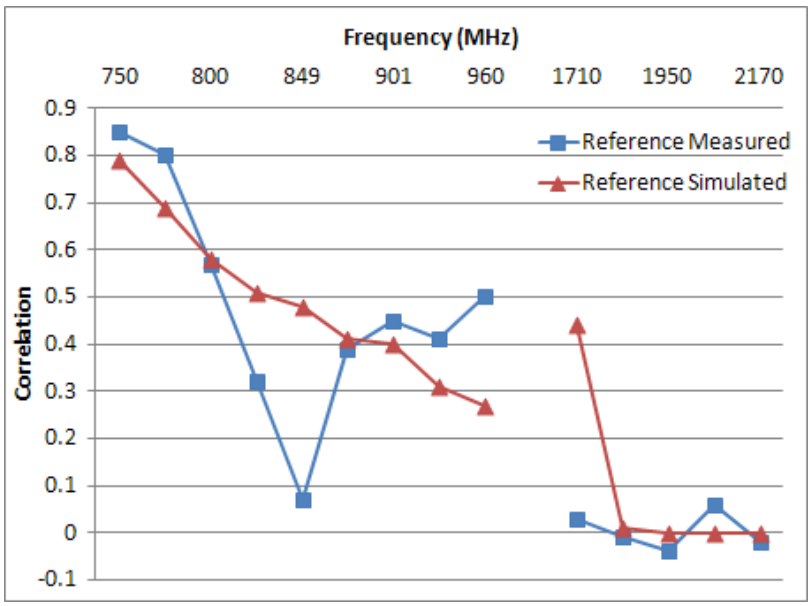

Figure 15. Reference Design Correlation

3.3.6 Multiplexing Efficiency

Using the Multiplexing Efficiency Equation (2), the equivalent loss of theoretical system capacity as expressed in dB is calculated for both the simulated and measured designs and pictured in Figure 16.

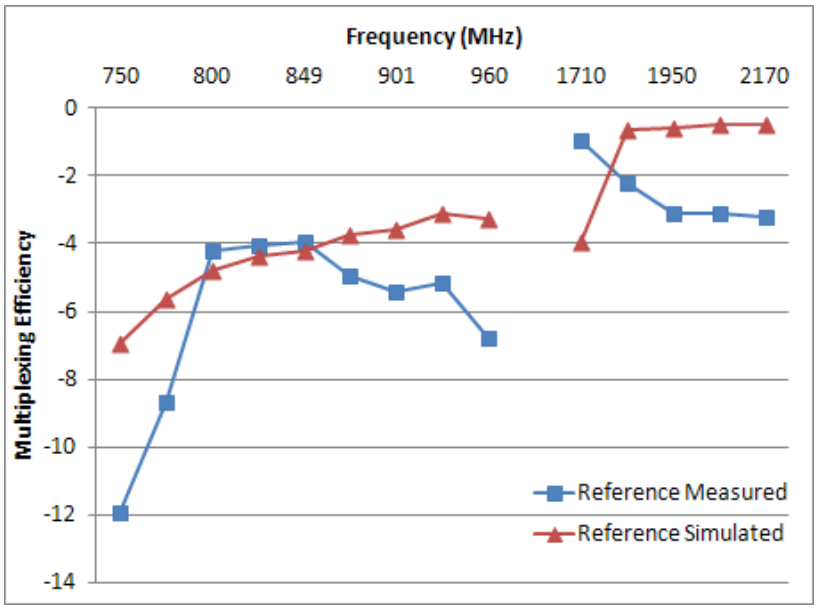

Figure 16. Reference Design Multiplexing Efficiency

3.3.7 Battery Effects

An important parameter to examine when developing a phone is the response of the antennas when a battery is added. The sizable chunk of metal (i.e., battery) will reduce the antenna efficiency, and may be a deciding factor when choosing between designs.

A 50 mm x 50 mm x 4 mm block of copper that represents the battery was added in the simulations in two different positions. One immediately adjacent to the bottom of the phone next to the antennas, and in another simulation it was moved 5 mm away from the antennas. The resulting antenna efficiencies were compared with the baseline results. This comparison is shown in Figure 17 below.

Predictably, the battery degrades the antenna efficiency. Adding additional spacing may increase the total length of the design and any size versus performance tradeoffs must be examined carefully.

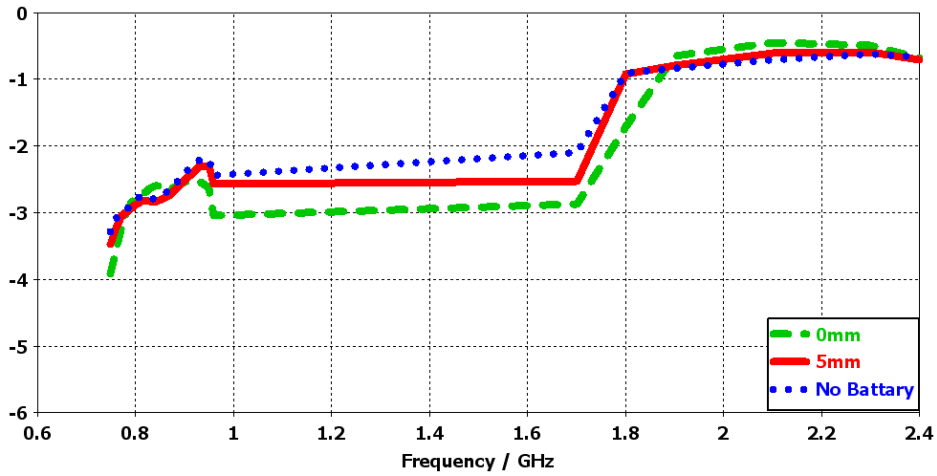

Figure 17. Reference Design Efficiency with Battery

3.4 Conclusions

This reference design illustrates the idea that a pair of "co-located" antennas can be a valid choice for handset design, even for a phone targeting an ambitious number of frequency bands down into the 700-MHz range currently allocated for LTE.

The clearance and board height may not be limiting factors; however, we have found through simulations that the width of the board is an extremely important constraint. The difference between a 60-mm width and 66-mm width can be crucial in the ability to design dual antennas with sufficient efficiency and envelope correlation in the lowband.

As expected for this design, the two most difficult specifications to achieve are the isolation and correlation at the lowest frequency band.

CHAPTER 4

4 L-fed

4.1 Theory and Background

The inductively fed (L-fed) concept used as a baseline for this design was developed primarily by Sony Mobile Antenna Engineer Rune Sø.

The feed creates a magnetic loop by running along a trace into the ground plane, which forms a magnetic coupling with a parasitic element extending out from the ground plane. The extension from the ground plane branches out into two sections, the lengths of which are carefully controlled to tune the antenna to two frequency bands to create a dual-band antenna.

The structure is pictured in Figure 18. As with the reference design some of the details are simplified.

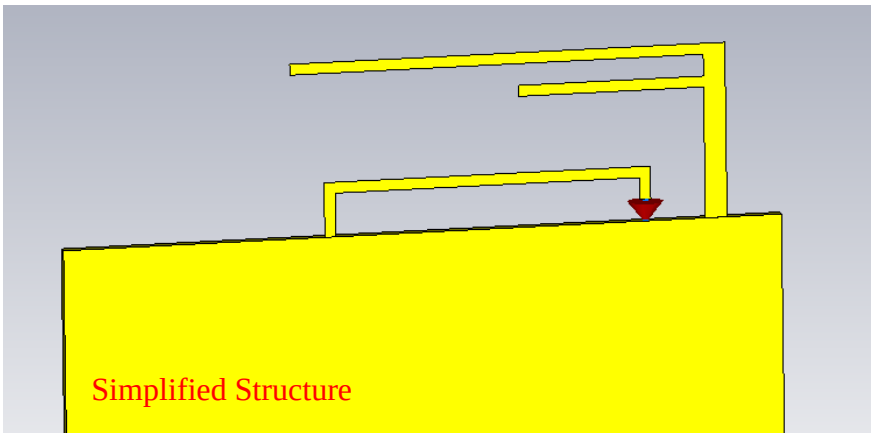

Figure 18. L-Fed Original Structure

The dimensions for this design are presented in Table 4.

TABLE 4. L-FED DIMENSIONS

Antenna Parameter	Length in millimeters
Antenna Total Length	41
Clearance (above board)	6
Clearance (out from board)	6

One of the biggest advantages of this design is that it is easy to modify to adjust the frequencies and bandwidth. The design covers the GSM bands listed in Table 1, as well as the HSPA band. It does not cover any of the three 700-MHz LTE bands.

The frequency response before matching is illustrated below in Figure 19.

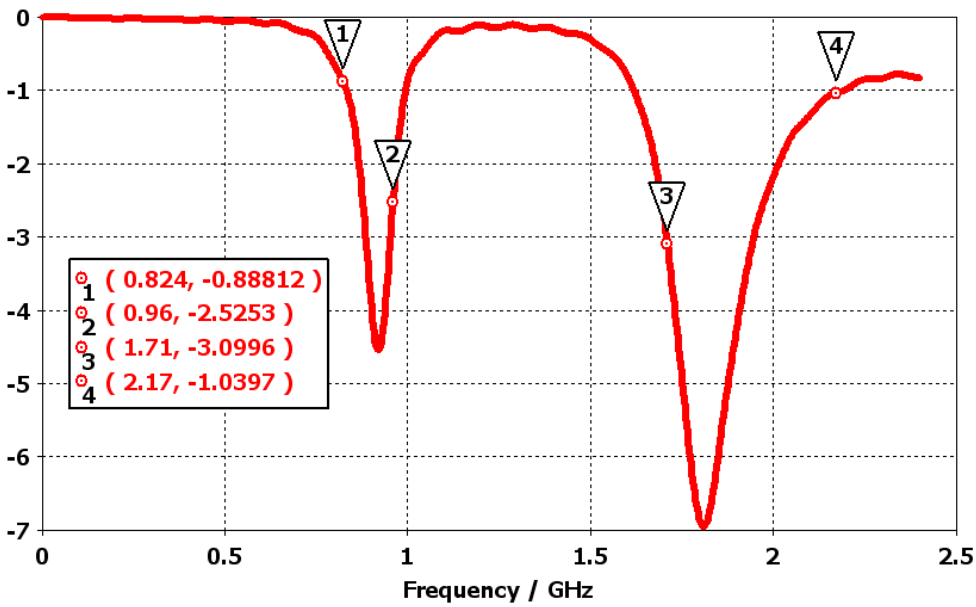

Figure 19. L-Fed Pre-match Reflection Coefficient

To understand this design, a visualization of the Smith chart is absolutely critical. There are two distinct loops, one for the lowband resonance and one for the highband resonance. A Smith chart showing the response of the design before matching is illustrated in Figure 20. With matching, they can be wrapped around closer to the center, as pictured in Figure 21.

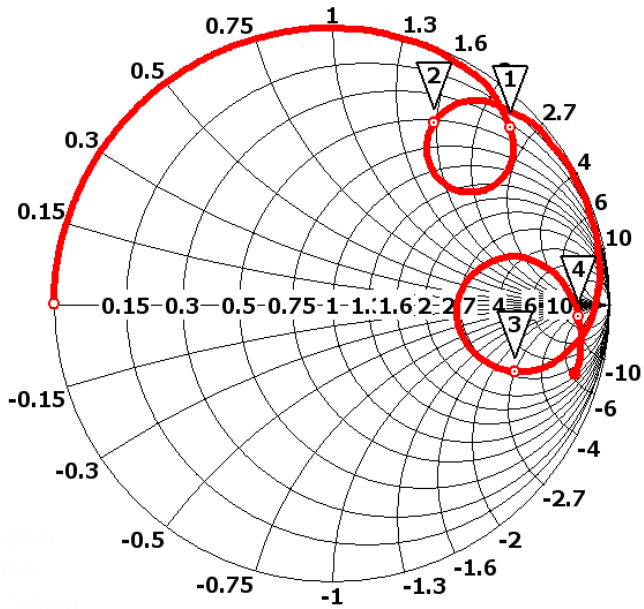

Figure 20. L-Fed Original Design Smith Chart (No Matching)

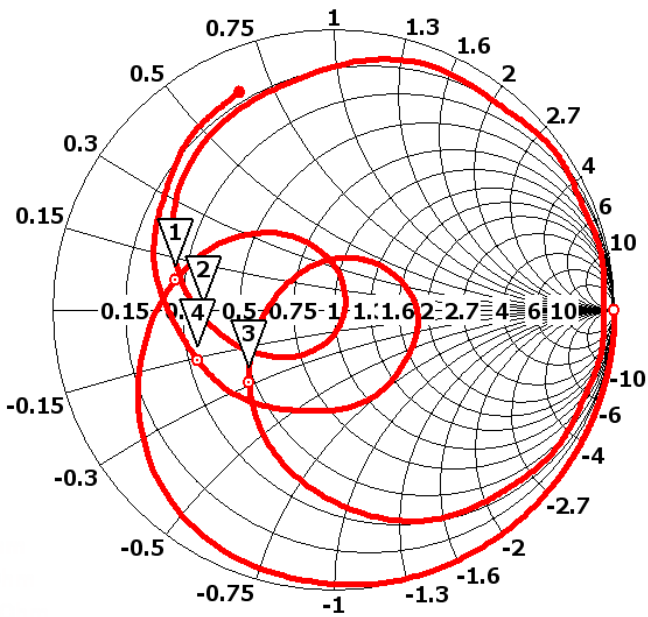

Figure 21. L-Fed Matched Smith Chart

It is critical to keep these loops in approximately the same location and diameter if the structure is adjusted. If they become too large, matching may be ineffective because it will not be possible to wrap them tightly around the center. If they are too small, they will become very sensitive to manufacturing tolerances and hand effects.

Adjusting almost any parameter of the design will affect these shapes. The next section provides the intuition into how adjusting each important dimension of the antenna will affect the frequency and phase response.

The far-field response is shown in Figure 22 for the center frequencies of the lowband and high bands.

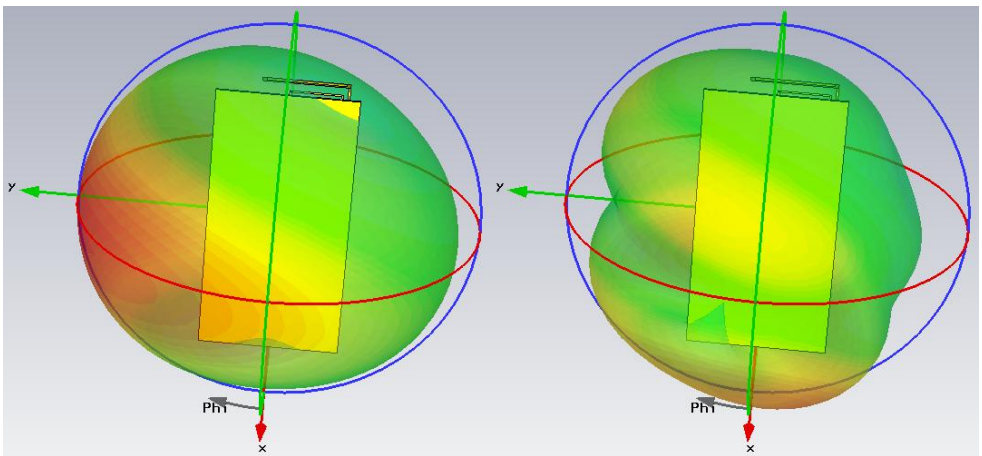

Figure 22. L-Fed Original Far-field Lowband (left) Highband (right)

4.2 Shrinking and Mirroring of the Structure

A co-located version of this design requires a significant reduction in the maximum dimension of the antenna—the length of the parasitic. The original antenna spans 41 mm, so a significant reduction is necessary to bring it down to half or even less of the board width.

Reducing an antenna's size necessarily requires tradeoffs in bandwidth and efficiency [6]. The goal is to reduce the structure as much as possible while still staying within the wireless operator specifications for each parameter.

4.2.1 Understanding Parameter Changes

To reduce the overall antenna size, it is critical to understand the impact of each part of the antenna structure on the system performance. An analysis of critical antenna dimensions follows.

Moving the Antenna along the Board Edge

The distance of the antenna from the board edge is critical for the bandwidth of the highband. Moving the structure closer to the edge narrows the highband response but has almost a negligible effect on the lowband. This will be an extremely important observation when the mirrored structure is introduced in the next section. Figure 23 illustrates this effect.

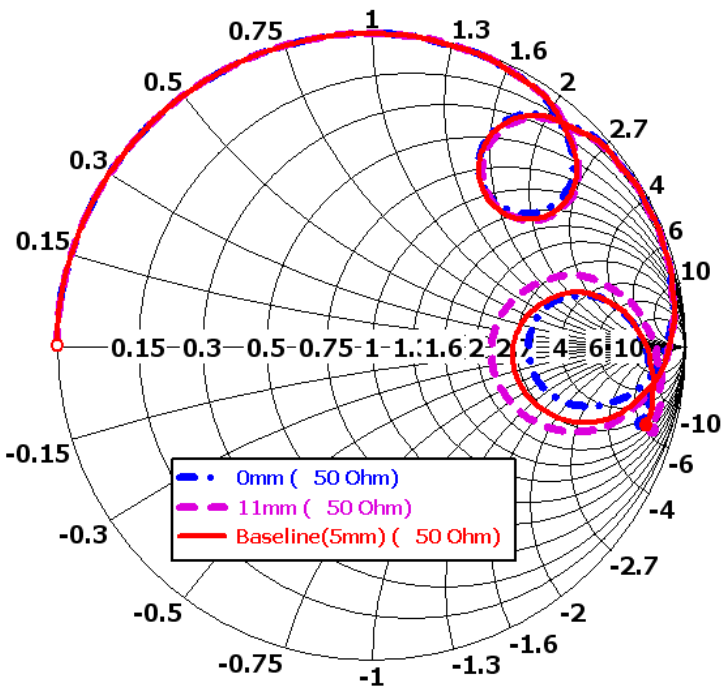

Figure 23. Parasitic and Feed Adjustment

Adjusting the Feed Dimensions

The feed is a very sensitive part of the design. The width and length of the inductive loop are critical for determining the frequency response and

bandwidth. As a general rule, the height of the feed will be proportional to the circumference of the pre-matched loops from Figure 20.

The length of the feed will rotate the response around the Smith chart. Adding length rotates the response clockwise, and shortening the feed rotates the response counter-clockwise, as illustrated in Figure 24.

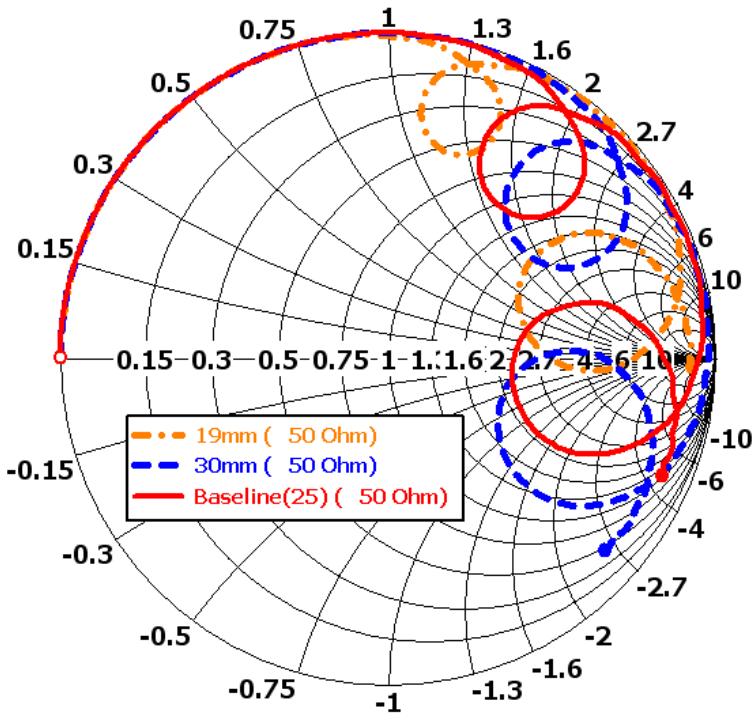

Figure 24. L-Fed Feed Length Adjust

Adjusting the Parasitic Branches

The length of each branch is tuned to center one of the resonances. The longer branch sets the lower resonance (824-960 MHz) and the short branch sets the higher band resonance (1710-2170 MHz). Shortening either branch will raise the respective resonant frequency.

Changing the Meander Width / Spacing

Meander line is an effective tool for reducing the dimensions of an antenna. By cutting slots in the side of a structure, the path of the currents can be significantly increased in length [20]. The amount that the electrical length is increased is proportional to the total length that the currents must travel on the meandered structure.

However, while meandered structures offer more compact designs, the bandwidth will be reduced for the branch in which it is utilized.

Sensitivity to Board Width / Height Adjustments

The response is quite consistent when the length of the phone is increased or decreased, even by as much as 40 mm. The widths of the loops on the Smith chart change, but this can be compensated by adjusting the feed height.

The board width is a more sensitive parameter. Reducing the width of the board and keeping the feed and parasitic at the same relative distance to each side will shrink the lowband resonance and increase the highband resonance.

Increasing the Ground Clearance

The "Ground Clearance" is a measure of the separation of the antenna from the main ground plane and it is necessary for the antenna elements to radiate. Minimizing this parameter is desirable because it will add to the length of the phone, but to do so is challenging. In general, larger ground clearance leads to better bandwidth.

Process and End Result

After careful consideration of each of the parameters, an iterative process was employed to gradually reduce the total length of the parasitic by adding meander line to increase electrical length and expanding slightly in the other directions (clearance and phone thickness).

The mock-up is printed on a narrow piece of plastic with no cover, and simulation results show that adding a cover results in a further bandwidth reduction and a downshifting of the frequencies.

The parasitic length of the original design concept was reduced in 3-5 mm steps while adjusting the branch length, distance from the board edge, feed height, length, thickness, and ground clearance. The end result is shown in Figure 25.

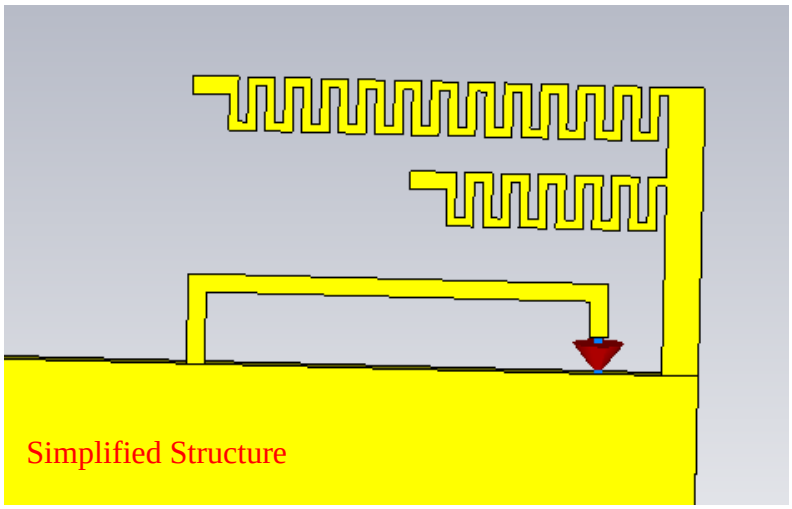

Figure 25. Shortened Version of Structure

The total dimensions are given in Table 5.

TABLE 5. SHORTENED L-FED DIMENSIONS

Antenna Parameter	Length in millimeters
Parasitic Total Length	29
Clearance (above board)	6
Clearance (out from board)	8
Feed Length	25
Distance from board edge to parasitic	0

The total parasitic length was reduced to 29 mm, at the expense of increasing the thickness of the phone by 2 mm. Several experiments were conducted to try to reclaim some of this space, and the results are detailed later in this chapter.

4.2.2 Mirroring the Structure

The first step was to mirror the structure and analyze the effect on the individual responses of each element. The element from Figure 25 was mirrored on the opposite side of the board.

There was an extremely strong interaction between the two elements. An additional lowband resonance was created at a lower frequency and the original lowband resonance was pushed up, which displayed itself as a double-curl on the Smith chart, illustrated in Figure 26 below.

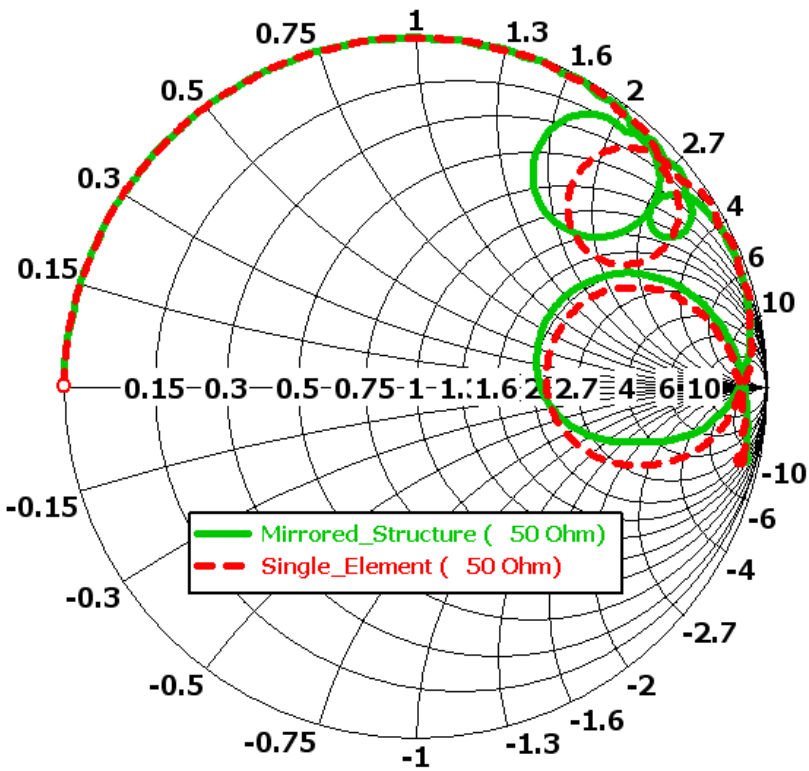

Figure 26. Smith Chart for the Mirrored Structure

When the two elements are narrowly spaced, isolation becomes an absolutely critical parameter. Currents from one feed can be coupled to the other in a variety of ways with a narrowly spaced geometry, and there are a number of techniques to reduce this coupling [21].

The isolation in this configuration was found to be extremely poor to the point of rendering it unusable. CST-generated Figure 27 below shows isolation values in the range of 3-4 dB, and measured mock-ups yielded even worse isolation values of 2-3 dB.

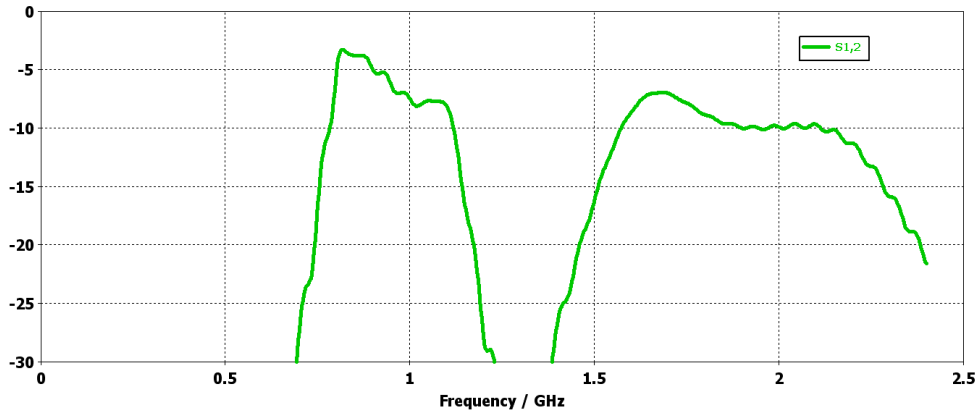

Figure 27. Mirrored Structure Coupling Coefficient

Several experiments were conducted to try to improve this isolation. A hole was cut in the ground plane in an attempt to increase the distance between the feeds along the top of the board, as shown in Figure 28.

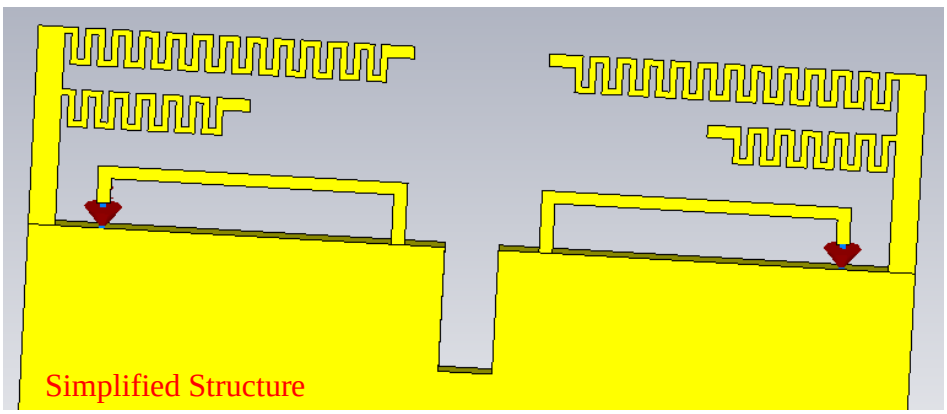

Figure 28. Mirrored Structure with Ground Plane Cut

The hole in the ground plane proved to have a negligible effect on the response. Even if it had yielded useful results, this method may not be a viable solution for a production design because the battery would be placed in this section, which could short the gap regardless.

Another experiment involved adding a neutralization line to connect the parasitics in an attempt to reduce the coupling between the two sides, as shown in Figure 29.

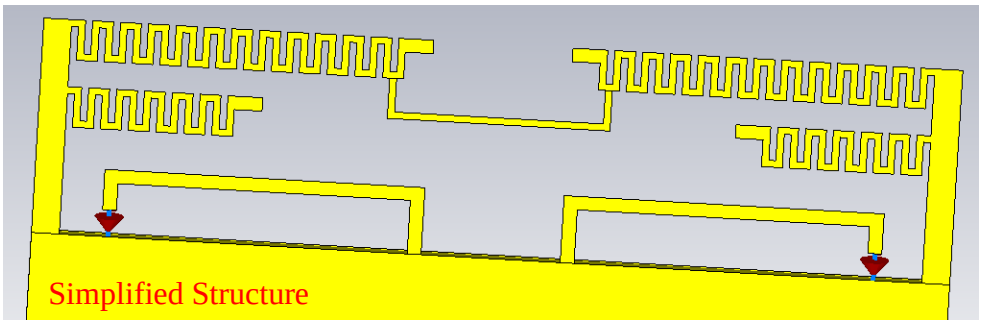

Figure 29. Mirrored with Neutralization Line

Many variants of the neutralization line were tested both through simulation and with lengths of wire on the physical board. Several of the variants were successful in reducing or eliminating the additional lowband curl in the Smith chart, but no line or combination of lines was successful in achieving the dual-band improvement in isolation required to reduce the isolation to an acceptable value.

With no success in improving the isolation on the mirrored structure, the design was modified in a more fundamental way. Each of the two sides was flipped to move the feeds and the ground connection to the parasitic to the inside of the board.

An example of this configuration is shown in Figure 30.

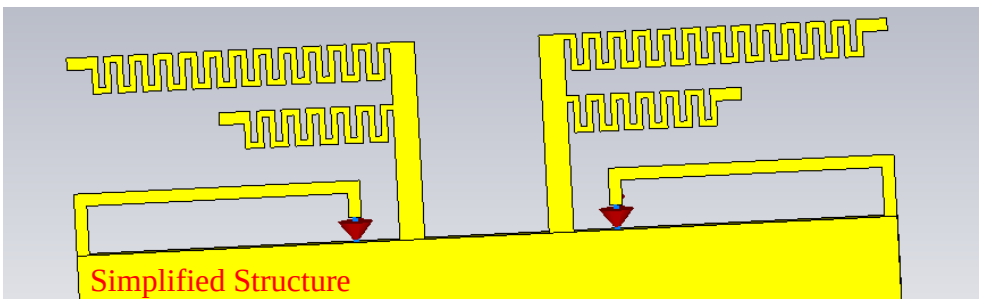

Figure 30. Mirrored and Flipped Structure

As the edge of the highband branch gets closer and closer to the edge of the board, the response on the Smith chart becomes very wide and disproportionate to that of the lowband, as shown in Figure 31. When this ratio becomes too disproportionate, no matching circuit is able to wrap both branches around the center for an acceptable response. No combination of adjusting the feed dimensions or increasing the clearance proved successful for tuning the response back to the original configuration, even when an iterative approach was taken to reduce the structure step-by-step.

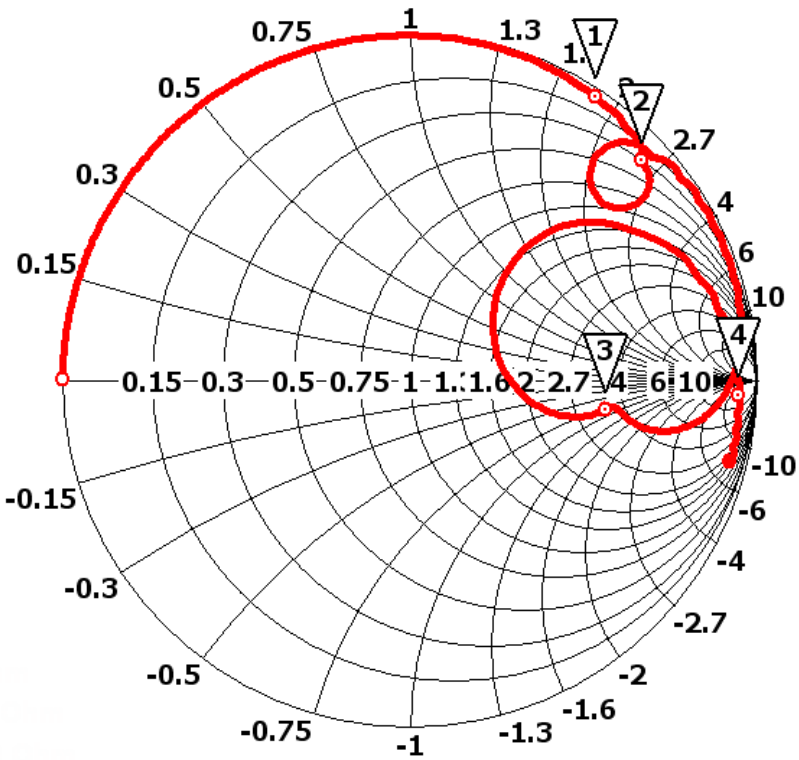

Figure 31. Mirrored and Flipped Structure Smith chart

One more modification was made to the "flipped" design to fix the frequency response and bring it back to close to the original design. The location of the lowband and highband parasitic branches was reversed.

The length of each branch, along with the meander size and spacing, was adjusted iteratively in the same process as before, starting with a full 41

mm and reducing in steps until the design converged to the configuration shown in Figure 32.

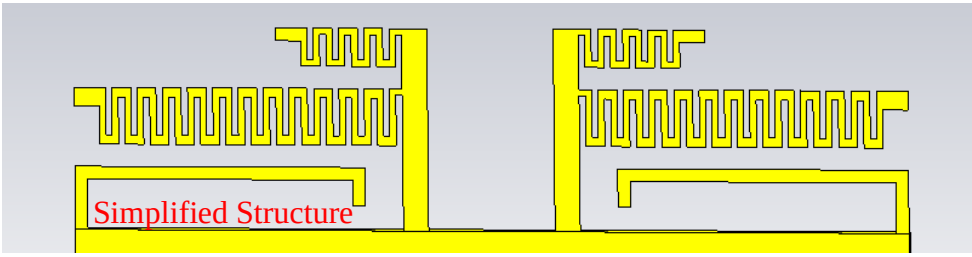

Figure 32. Mirrored, Flipped, and Reversed Structure

The short branch was bent into an "L" shape and no meander was necessary to achieve the necessary electrical length. The long branch, however, consists entirely of meander line.

4.3 Results of Final Design

The final design in Figure 32 was optimized extensively in simulation, and a prototype of the design was constructed and tested against the simulated results.

4.3.1 Return Loss

The reflection coefficient of the final, matched design is shown below in Figure 33. It meets the return loss requirements across the desired bands, but quite narrowly.

The measured frequency response from the prototype is shown in Figure 34. The bandwidth is narrower than that of the prototype, partially due to cable losses, dielectric losses, and partially due to the imprecision of the design in the mock-up stage.

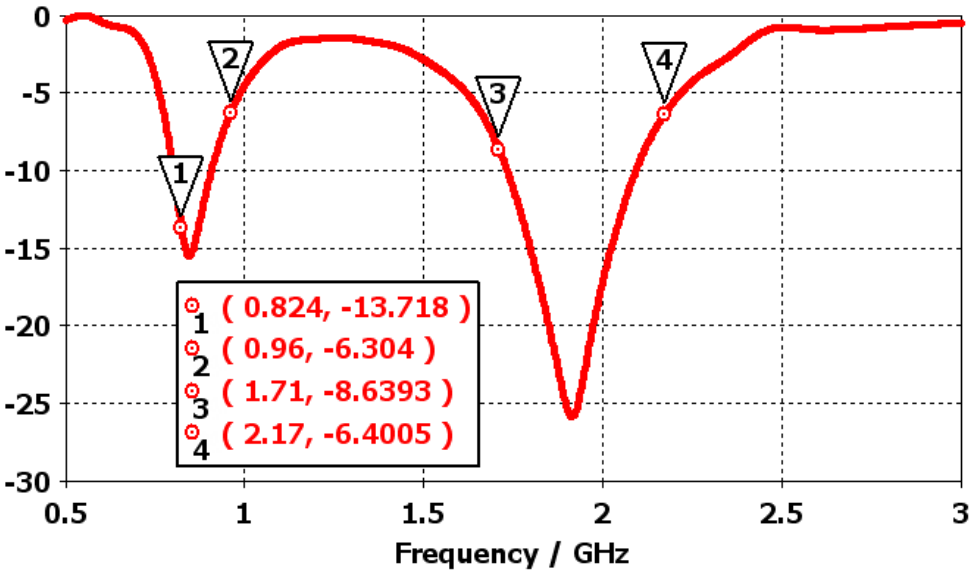

Figure 33. Simulated L-Fed Reflection Coefficient

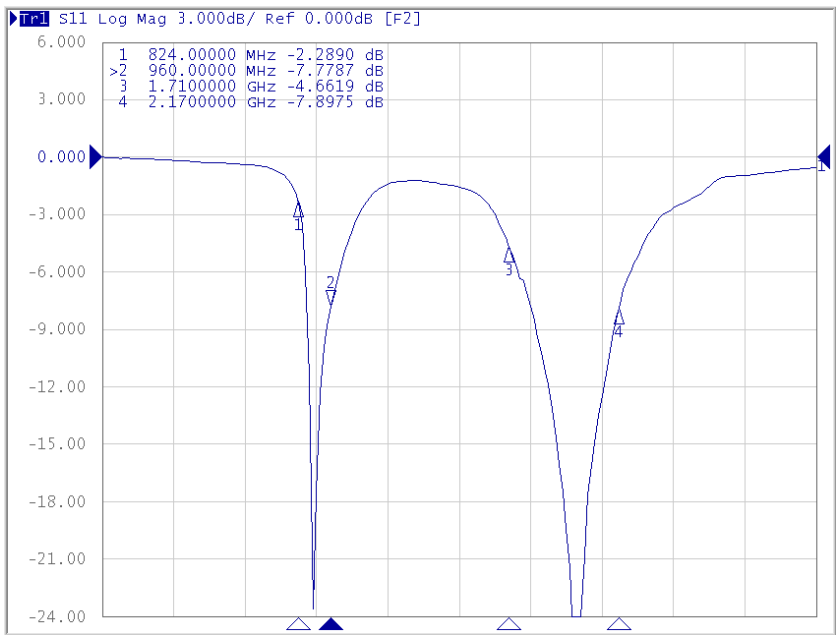

Figure 34. Measured L-Fed Reflection Coefficient

The Smith chart is not wrapped around the center quite as precisely as the original design (Figure 21), but maintains the same basic shape and is shown below in Figure 35.

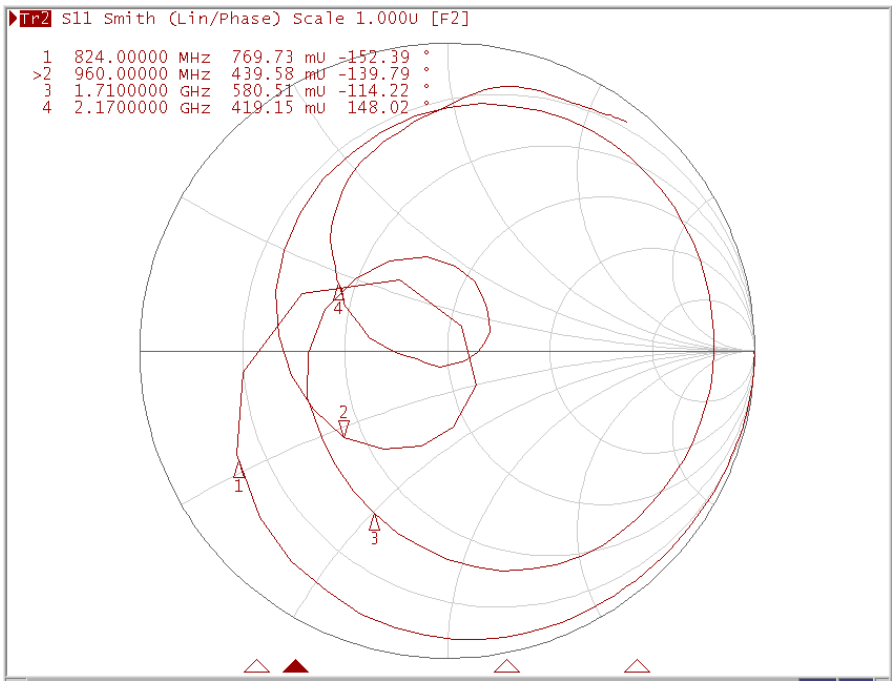

Figure 35. Measured L-Fed Smith chart

4.3.2 Isolation

The simulated isolation, displayed in Figure 36, is fantastic for this design. Across the bands the isolation is never lower than about 12 dB.

The measured isolation is shown in Figure 37. It bears a similar shape to the simulation, though the values are 1 to 1.5 dB higher. The minimum value is around 10.5 dB. One possible cause for the discrepancy is that the high current areas are heavily soldered with antenna connectors, matching components, and overlapping copper tape, which deviates from the smooth geometry of the simulation.

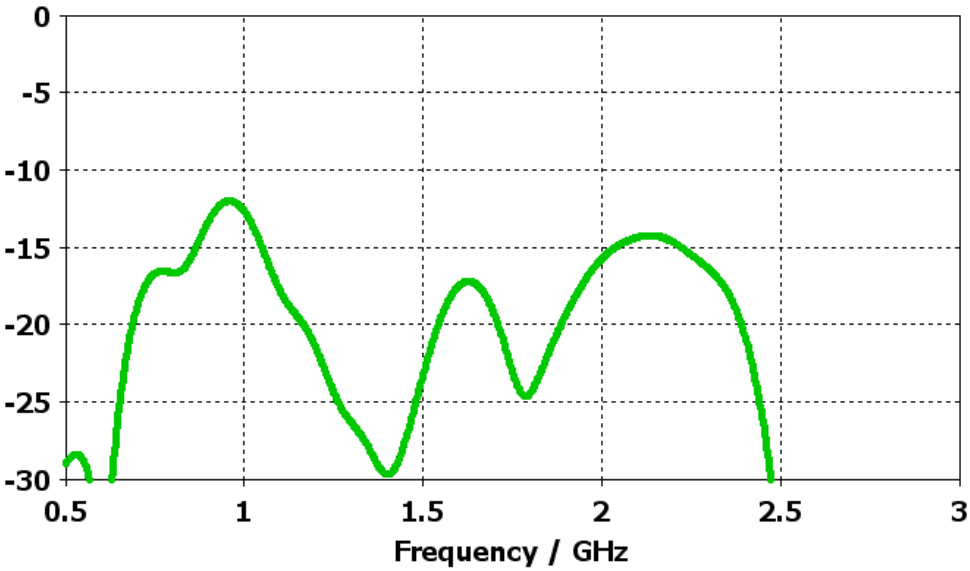

Figure 36. Simulated L-Fed Coupling Coefficient

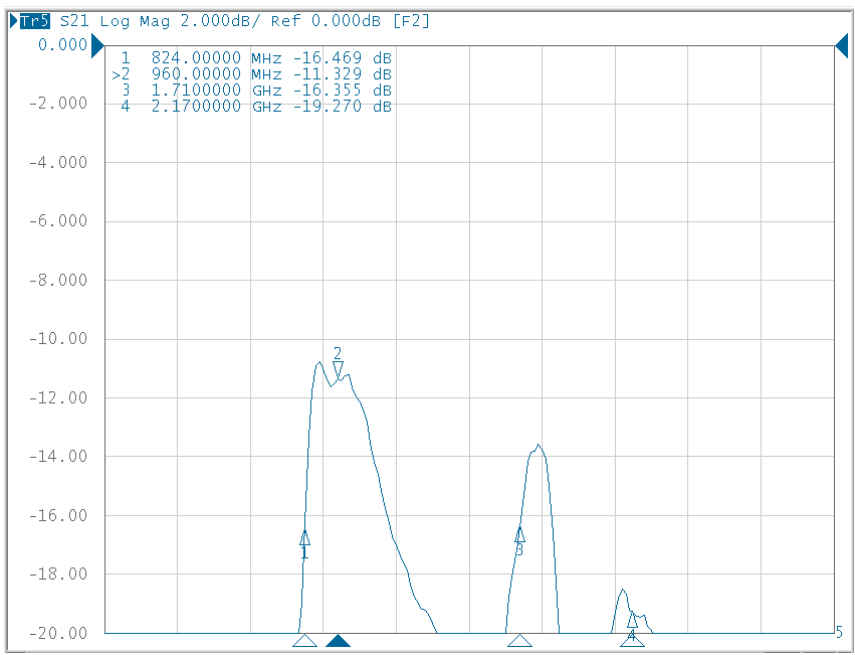

Figure 37. Measured L-Fed Coupling Coefficient

4.3.3 Efficiency

The efficiency is shown below in Figure 38. The free space efficiency design targets from Table 2 are almost met, but falling below the suggested -3 dB on the lowband edges in the simulation, and about 1 dB below for the measured case in the entire lowband, but it is always met with some margin for the highband.

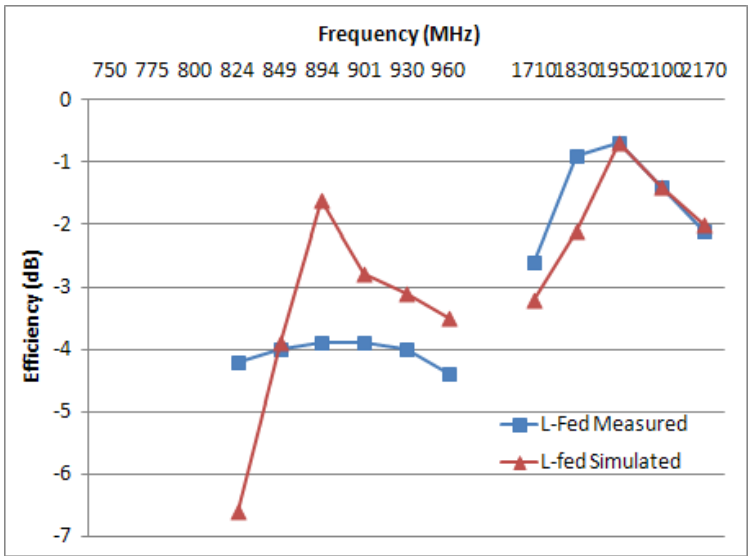

Figure 38. L-Fed Efficiency

4.3.4 Radiation Pattern

The simulated radiation pattern for the right-side antenna (right-side relative to Figure 32) is shown below. Notice that with the antenna elements reversed the radiation pattern main beam faces downward and to the right rather than downward and to the left.

The measured radiation patterns are displayed in Figure 40. The simulated and measured patterns resemble each other closely.

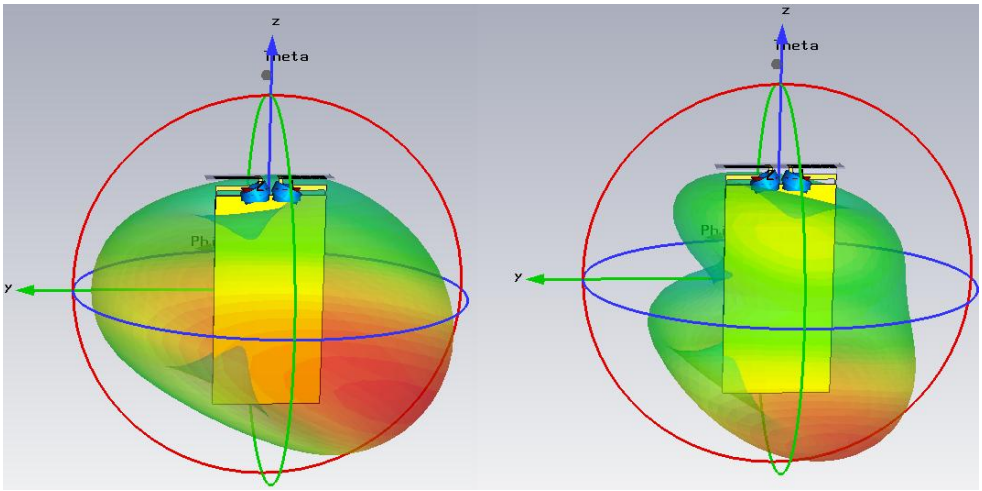

Figure 39. Simulated L-Fed Radiation Pattern for lowband (left) and highband (right)

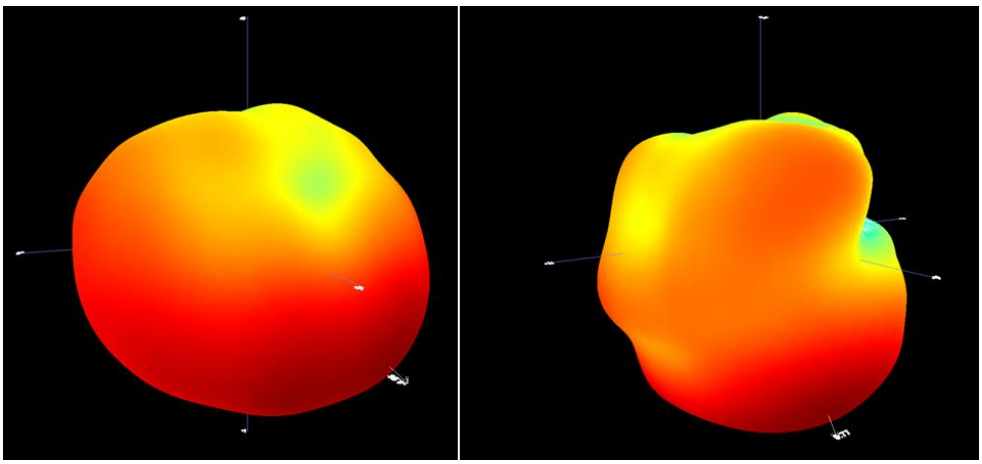

Figure 40. Measured L-Fed Radiation Pattern for lowband (left) and highband (right)

4.3.5 Correlation

The correlation is pictured in Figure 41. The simulation and measured results match very closely. The values exceed the specification of 0.5 at the lowest frequency. However because this design does not cover the LTE bands, the lowest frequency where correlation is specified will be the lowest downlink frequency, 869.2 MHz, where the design passes the requirement with some margin.

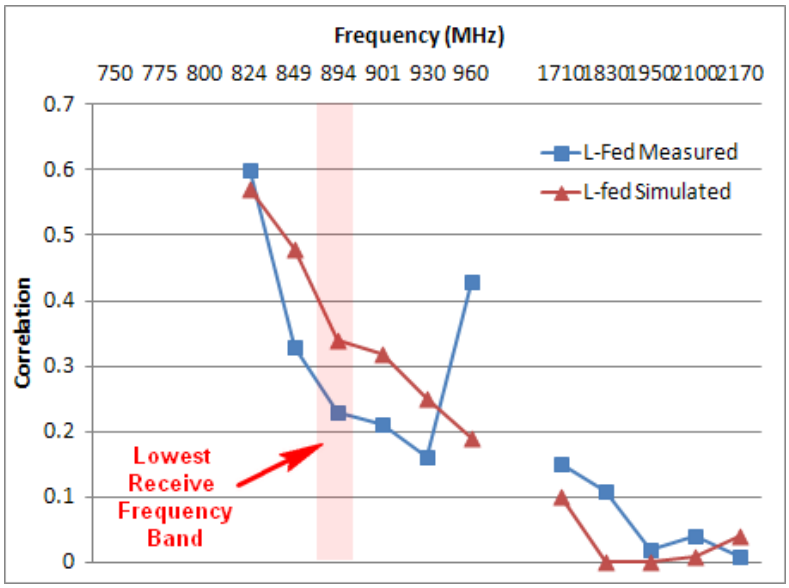

Figure 41. L-Fed Correlation

4.3.6 Multiplexing Efficiency

The multiplexing efficiency results are shown in Figure 43. The simulation and measured results match quite closely again. The results are dominated by high correlation in the lowband and efficiency in the highband.

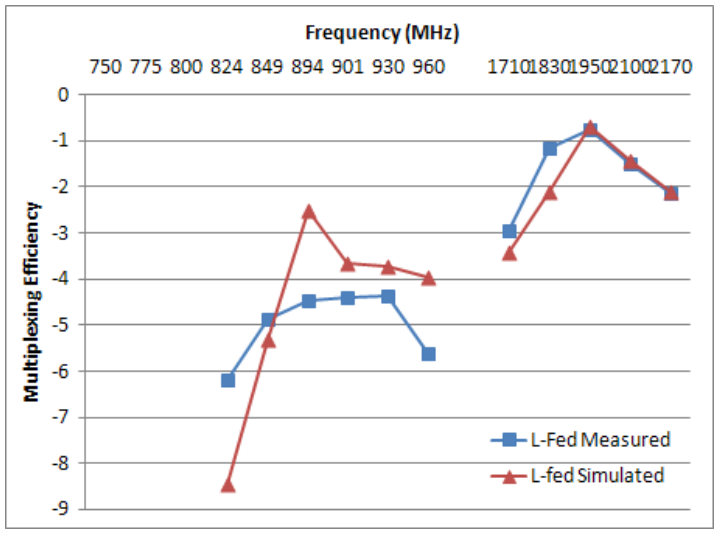

Figure 42. L-Fed Multiplexing Efficiency

4.3.7 SAR

A simulation of SAR was performed as shown in Figure 44. The results largely depend on the orientation of the device relative to the phantom head. A cross sectional cut is shown to illustrate the distribution on a 2-D plane.

Both ports were simulated at a range of frequencies averaging over 10 grams of tissue, and the results are presented below in Table 6.

TABLE 6. L-FED SAR SIMULATION

Frequency (MHz)	824	960	1710	2170
Port 1 SAR (W / kg)	0.57	0.29	1.99	1.55
Port 2 SAR (W / kg)	0.6	0.4	1.28	1.06

Figure 43.

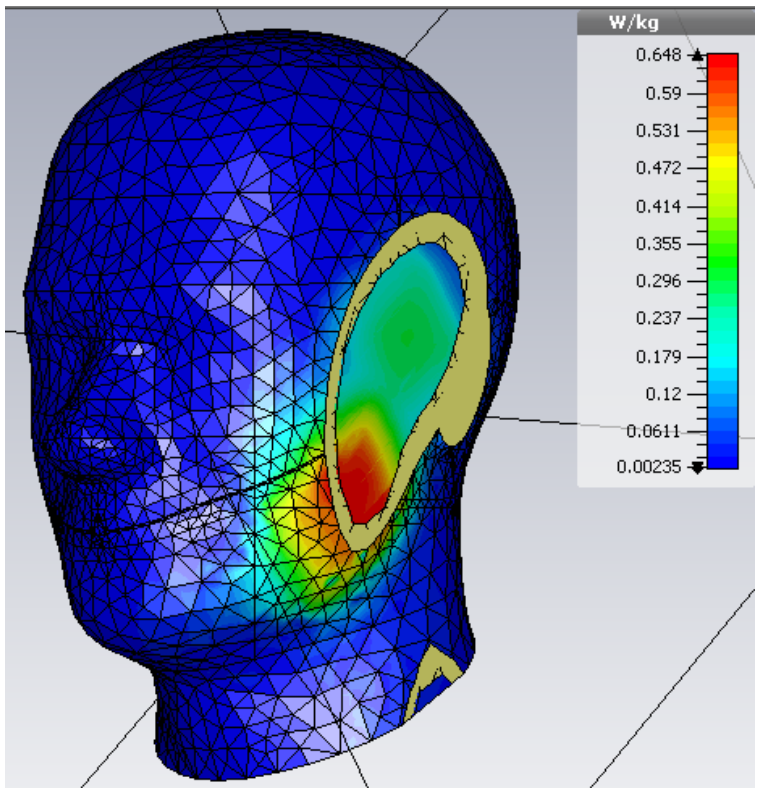

Figure 44. Simulated L-Fed SAR

4.3.8 Battery Effects

A battery was added in the same configuration as the reference design to gain an understanding of how what effect this would have on the antenna efficiencies. The results are shown in Figure 45. The design suffers a noticeable loss in efficiency, especially in the lowband when the battery is added with narrow spacing.

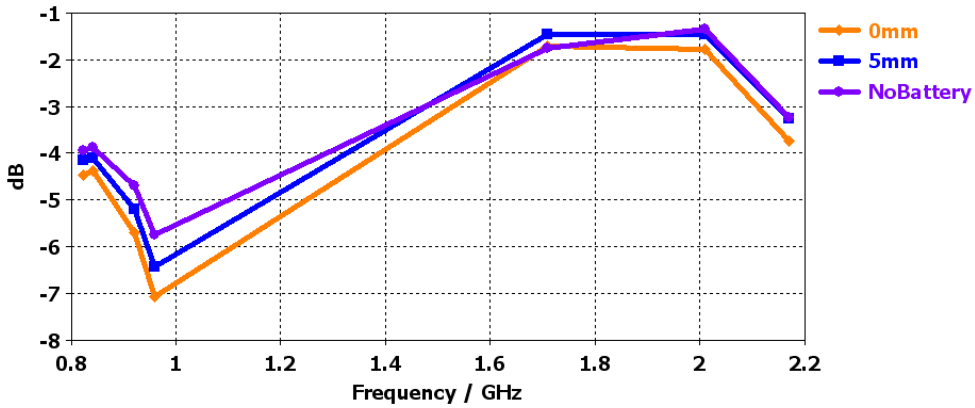

Figure 45. L-Fed Battery Effects – Original Matching

4.3.9 Effect of Curving / Bending the Parasitic

To fit the slim form factor of a phone, an antenna structure may not realistically span the full 10 mm allocated so far. Additional simulations replicated this curving along the back cover to determine the impact on the structure, as was done in the original single-element design.

Another series of experiments involved bending the structure around a carrier. The results are not included in this report, but in both instances the antenna bandwidth takes a significant hit, a very unfortunate consequence for a design already short on bandwidth.

4.4 Conclusions

The results show that an impressive isolation of at least 12 dB can be achieved even with very narrow spacing because of the way the current distributions are laid out. However, the bandwidth is very limited for this design, and compacting the design further from a mock-up to an actual phone would tend to reduce this bandwidth even more.

This design has potential for a phone with receive diversity only that does not extend into the 700 MHz band. The two antennas could maintain the same operating principles but the primary transmit and receive antenna could have the bandwidth extended.

CHAPTER 5

5 C-fed

5.1 Theory and Background

The capacatively fed (C-fed) dual band antenna presented here is based on an antenna concept developed by Sony Mobile Antenna Engineer Scott Vance and is pictured below in Figure 46.

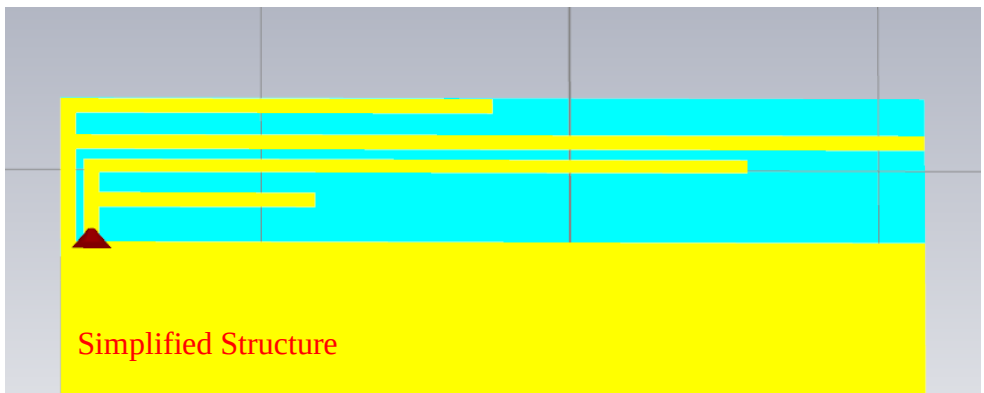

Figure 46. Original C-Fed Design

The antenna is a dual-band monopole consisting of a “driven element” along with a “parasitic element” extending from the ground plane to create a dual-band excitation. Each branch of the driven element couples with each branch of the parasitic element to create two highband and two lowband resonances.

The longest dimension of the antenna is dictated by the center frequency of the lowest desired resonance. A quarter-wavelength monopole with resonant frequencies centered at 800 MHz will have a total length of 93.7 mm.

The total dimensions are shown in Table 7.

TABLE 7. ORIGINAL C-FED DIMENSIONS

Antenna Parameter	Length in millimeters
Total Antenna Length	55
Clearance (Above Board)	6
Clearance (Out from Board)	5.8

This antenna covers all of the bands listed in Table 1, as low as 704 MHz.

5.2 Shrinking and Mirroring of the Structure

To reduce the size of the antenna, the original structure is folded around three sides of a rectangular cuboid (i.e., antenna carrier) with a relative dielectric constant ε_r of 4.4. The high dielectric constant of this carrier introduces loss and shifts the resonant frequencies downward. The additional losses are unfortunate, but shifting the frequencies down is a useful effect when the design is limited to a smaller geometry.

Bending the microstrip line around three different surfaces of the carrier, the total length is around 81 mm, close to the theoretical quarter-wave monopole length of 93.7 mm.

The physical size of the antenna is crucial, so folded conductive strip lines are used to reduce the volume occupied by the antenna. This provides one additional benefit of reducing the antenna Q-factor [22], [23], which is inversely proportional to its fractional bandwidth [22]. Altering the structure to occupy a smaller volume actually improves the bandwidth [24].

The optimization process was performed mostly manually. The branches of the original design were wrapped in various configurations around the carrier in an attempt to reduce the physical size. Initially, the shell dimensions were set at 6 mm x 6 mm x 30 mm.

5.2.1 Understanding the Parameter Changes

The critical dimensions become very apparent when reducing the geometry by wrapping the structure around the carrier and modifying the relative lengths, widths, and positions. Tuning each band was not a simple process, but some of the most critical parameters are described below.

Adjusting the Short Feed Branch

The shorter branch of the driven element is the primary control for tuning the highband resonant frequencies, but it also impacts the lowband frequencies. The thicker this short branch is, the better the highband bandwidth, as shown in Figure 47.

Adjusting the distance between this branch and the ground plane is another critical parameter. Closer spacing results in a tradeoff between the highband bandwidth and the lowband bandwidth, as illustrated in Figure 48.

Adjusting the Driven Element and Parasitic Element Spacing

The lowband is tuned primarily by adjusting the separation between the driven elements and the parasitic element. The closer the two are, the tighter the coupling between two branches and the lower the frequency response. Increasing the separation pushes the lowband response upward.

Figure 49 shows the return loss of the antenna for three different values of separation, and there appears to be a separation that optimizes the lowband bandwidth.

Adjusting the Branch Location on the Carrier

Strong currents flow in the long branches running along the carrier, and the positioning of these is also critical. This provides another mechanism for tuning the relative bandwidths of the high and lowband. Placing the branches closer to the ground plane provides additional bandwidth in the lowband, as illustrated in Figure 50.

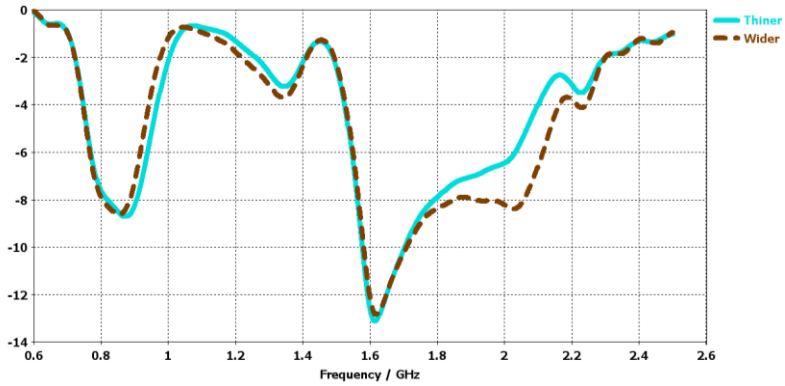

Figure 47. C-Fed Short Branch Thickness Comparison

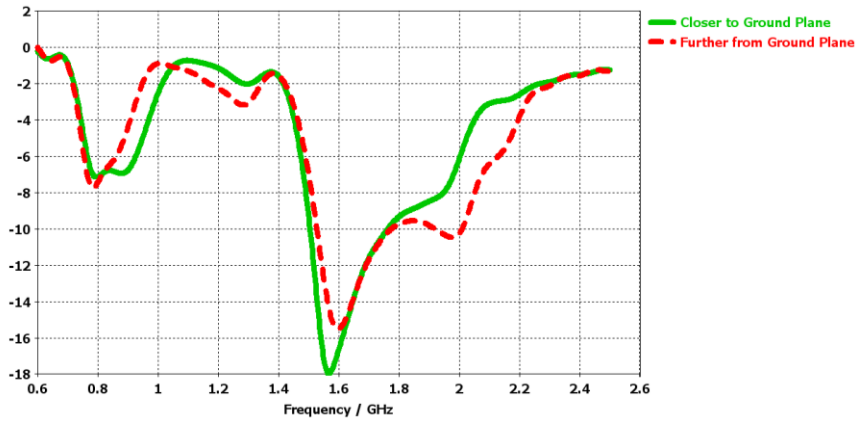

Figure 48. C-Fed Short Branch Ground Spacing Comparison

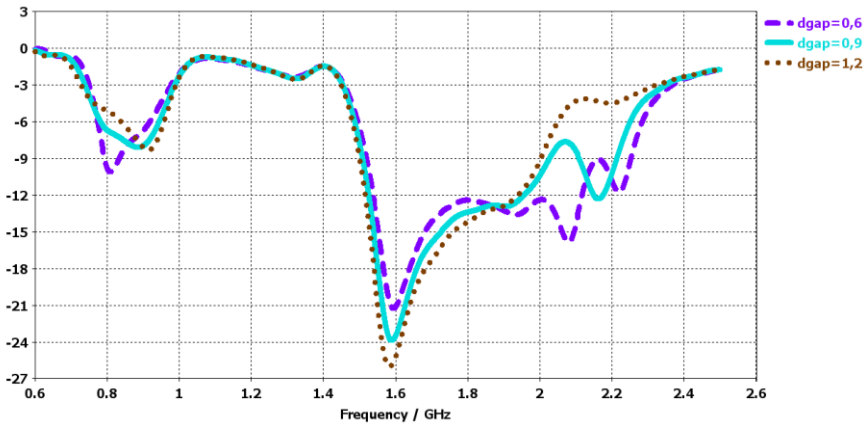

Figure 49. C-Fed Driven and Parasitic Element Spacing Comparison

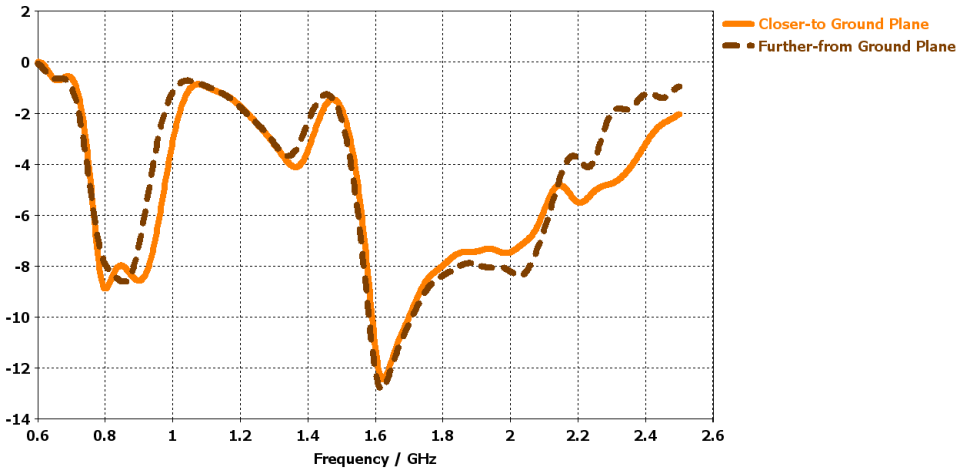

Figure 50. C-Fed Branch Location Comparison

5.2.2 Mirroring the Structure

When doubling the structure to create a co-located design, a "mirrored" version was first developed where the two elements had reflective symmetry across the middle of the board and were both fed from the outside, as shown in Figure 51.

The most difficult limitation when developing the two-antenna system proved to be the isolation between the two. This mirrored structure yielded isolation results that are similar to the reference design, i.e., around 6 to 7 dB at the minimum.

As with the L-Fed design, neutralization lines were tested extensively in an attempt to create an alternative current path in the opposing direction. Physical neutralization lines were connected using wire, co-axial cable, and copper strips with and without chip inductors. Other alternatives were simulated in CST. The results showed limited success in improving the isolation, and any gain was offset by the disturbance the extra copper caused to the antenna frequency response.

Other unsuccessful experiments conducted included adding a copper isolator/scattering mechanism between the antennas as per the reference design, and cutting a hole in the board.

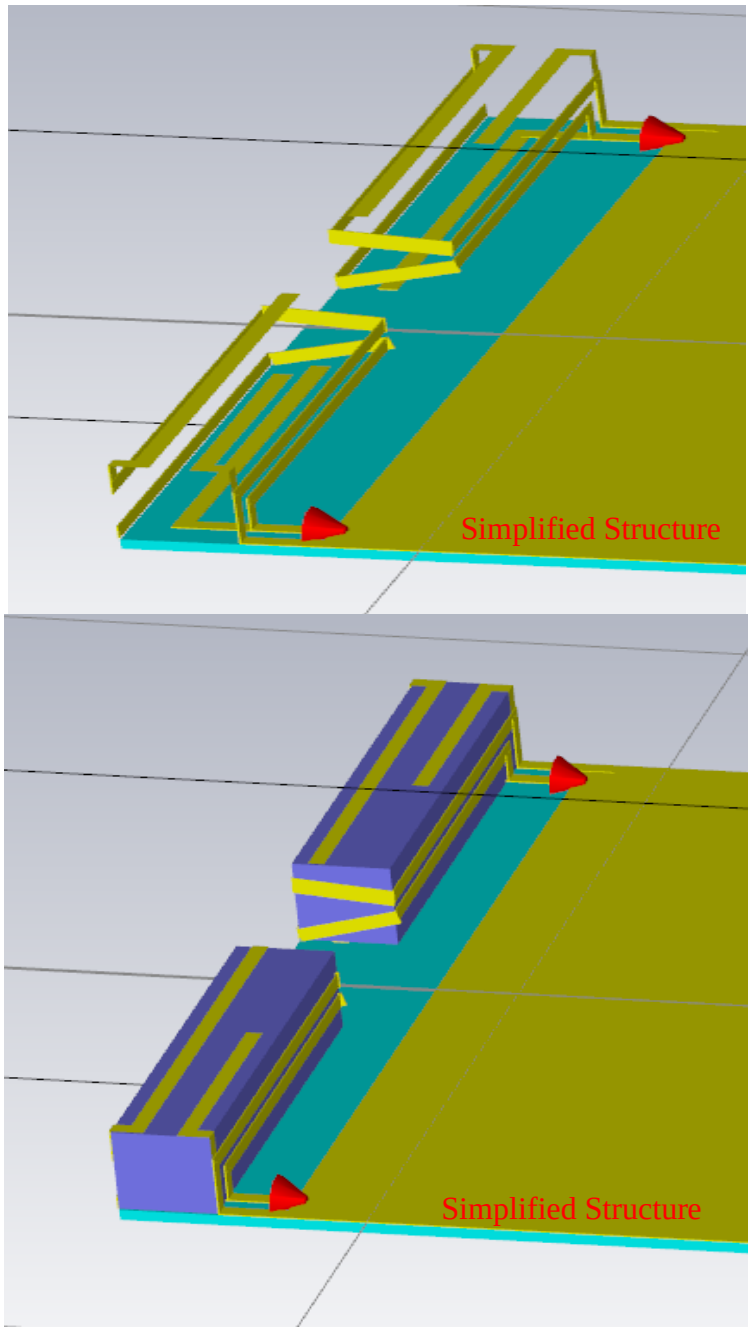

Figure 51. Mirrored C-Fed Configuration (shown with and without carrier)

A “duplicated” structure was developed where the elements each had the same orientation and were merely shifted to the other side of the board, as pictured in Figure 52.

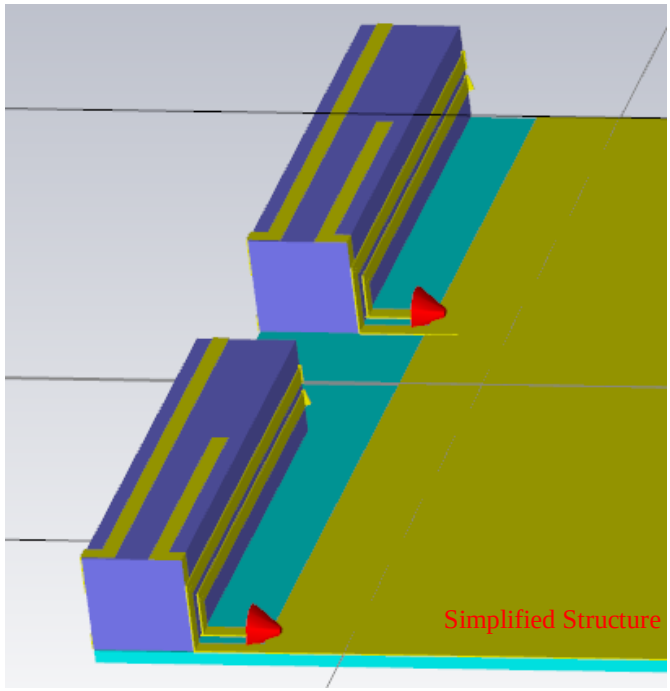

Figure 52. Duplicated C-Fed Structure

This structure showed promise for improving the highband isolation to acceptable levels, as seen in Figure 53, but the lowband isolation was identical or even slightly worse.

Furthermore, this improvement seems to have come at the cost of individual antenna element performance, as shown in Figure 54. An additional drawback to the duplication method is that the correlation looks to be worse than the mirrored model.

Given these results, the results in the following section are taken based on the final version of the mirrored design shown in Figure 51.

Finally, a matching circuit as pictured in Figure 55 was added to obtain another small boost in performance.

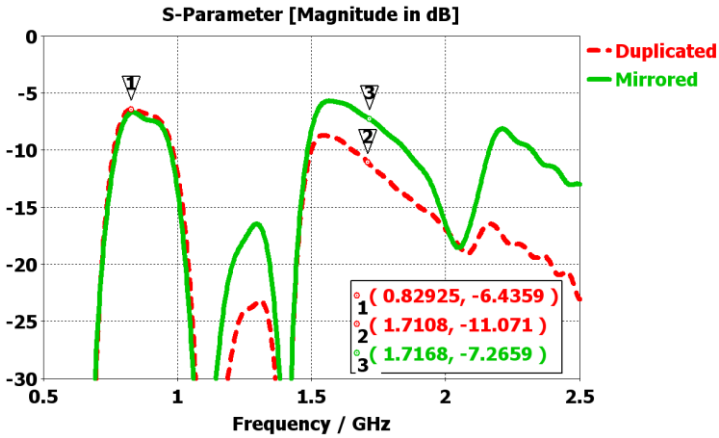

Figure 53. C-Fed Coupling Coefficient

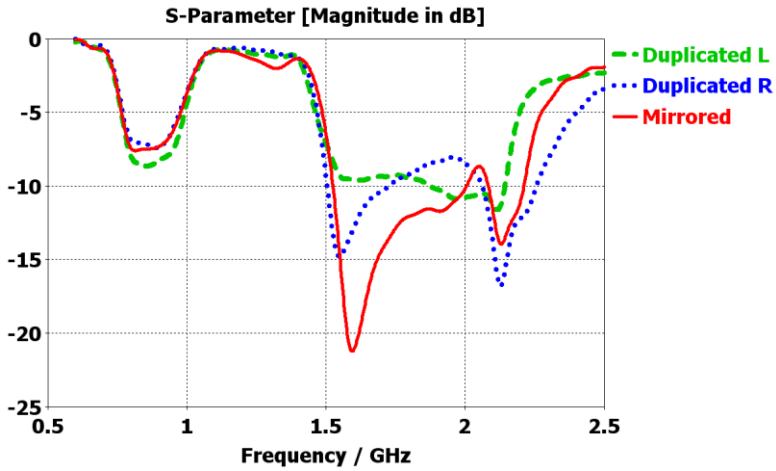

Figure 54. Mirrored vs. (Left/Right) Duplicated C-Fed Reflection Coefficient

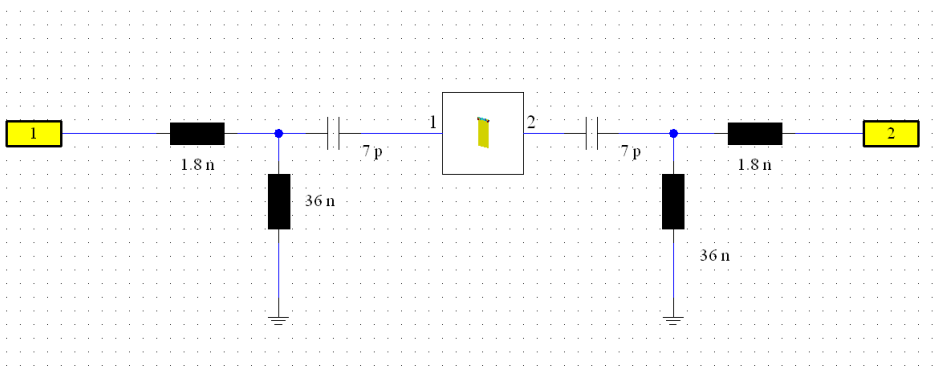

Figure 55. C-Fed Matching Circuit

5.3 Results of the Final Design

In addition to the optimized simulation of Figure 51, a mock-up of the design was created and the results were compared.

5.3.1 Return Loss

The reflection coefficients before and after the implementation of the matching circuit are shown in Figure 56.

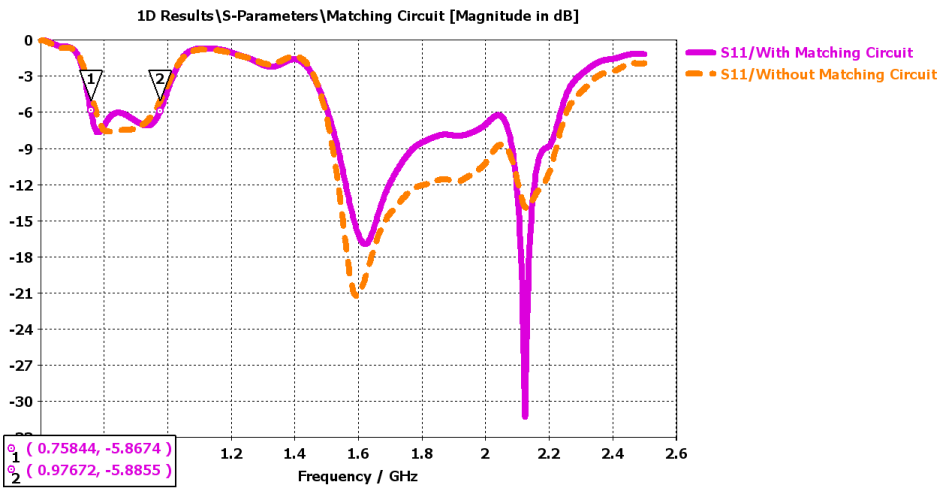

Figure 56. C-Fed Simulated Reflection Coefficient, before and after matching

The Smith charts before and after the matching circuit implementation are shown in Figure 57.

The measured reflection coefficient from the prototype is displayed in Figure 58.

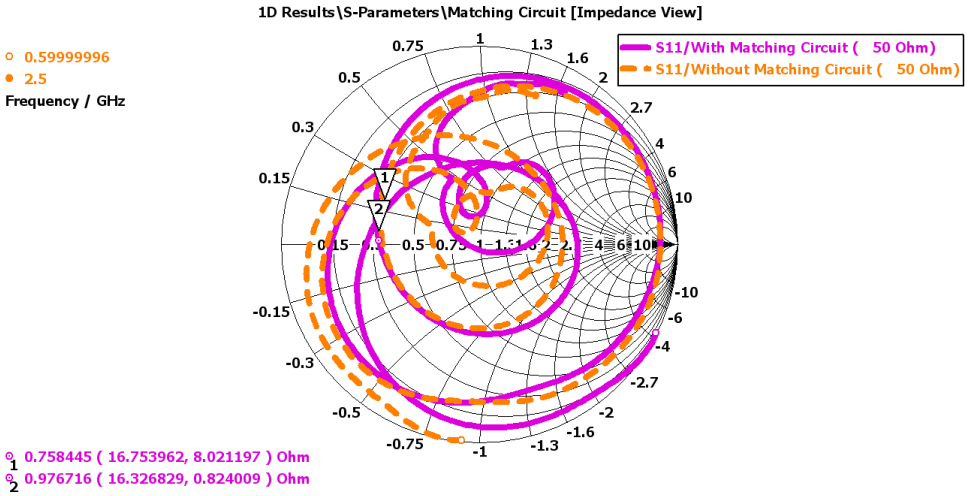

Figure 57. C-Fed Simulated Smith chart, before and after matching

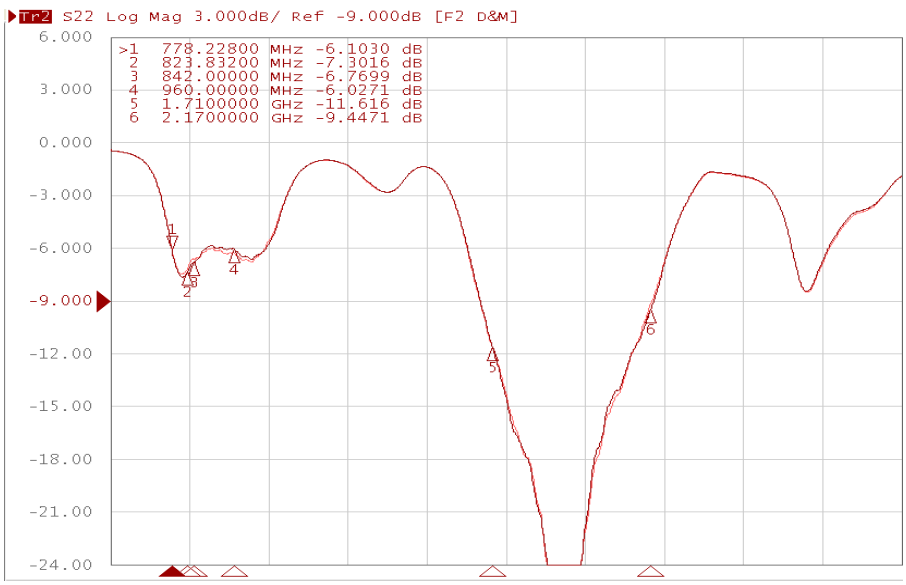

Figure 58. C-Fed Prototype Reflection Coefficient

5.3.2 Isolation

The coupling coefficients for the simulated duplicated and mirrored designs are shown in Figure 59.

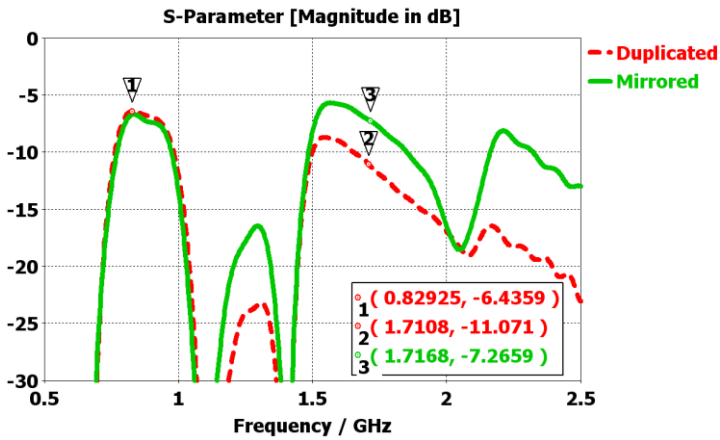

Figure 59. C-Fed Measured Coupling Coefficient

The measured coupling coefficient for the mock-up (mirrored) design is shown in Figure 60.

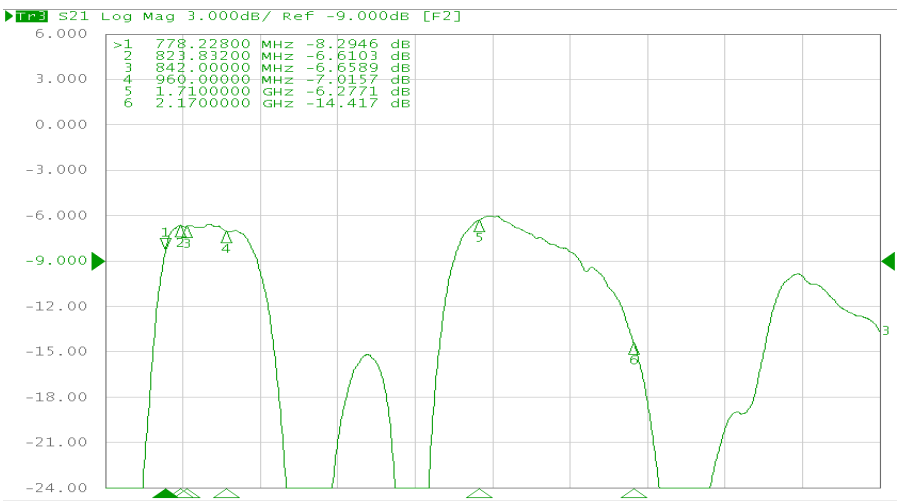

Figure 60. C-Fed Prototype Coupling Coefficient

5.3.3 Efficiency

The simulated and measured efficiencies are compared and shown in Figure 61. The results track each other quite closely, and fulfill the specifications except at extremely low and extremely high frequencies.

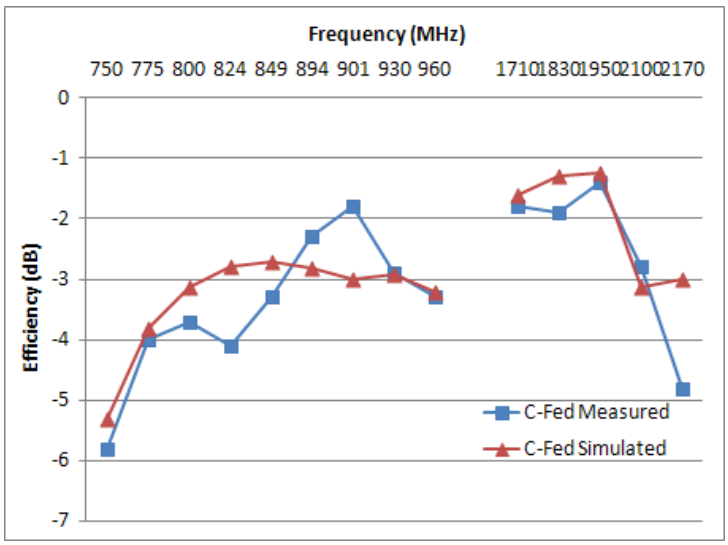

Figure 61. C-Fed Efficiencies

5.3.4 Radiation Patterns

The radiation pattern for the left-hand element is displayed in Figure 62. The lowband is less directive, with a pattern resembling a slightly rotated dipole. The highband is much more directive with the pattern pointing down and left.

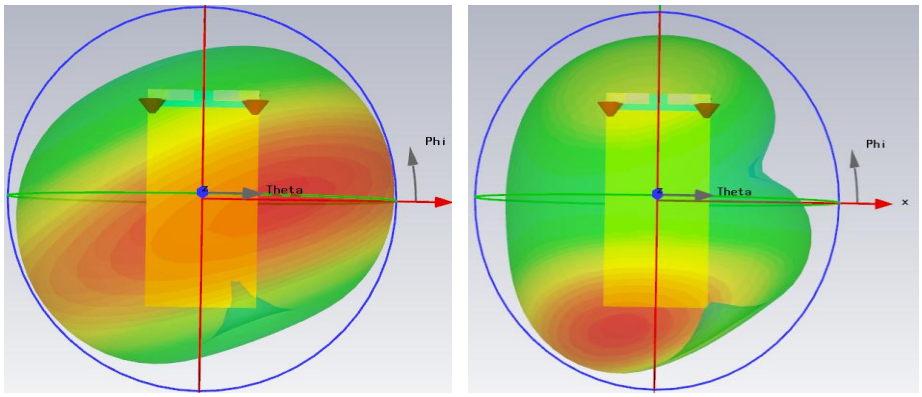

Figure 62. C-Fed Simulated Radiation Pattern at 850 MHz (Left) and 1950 MHz (Right)

As with the L-Fed, the measured results seem to match quite closely, as shown in Figure 63.

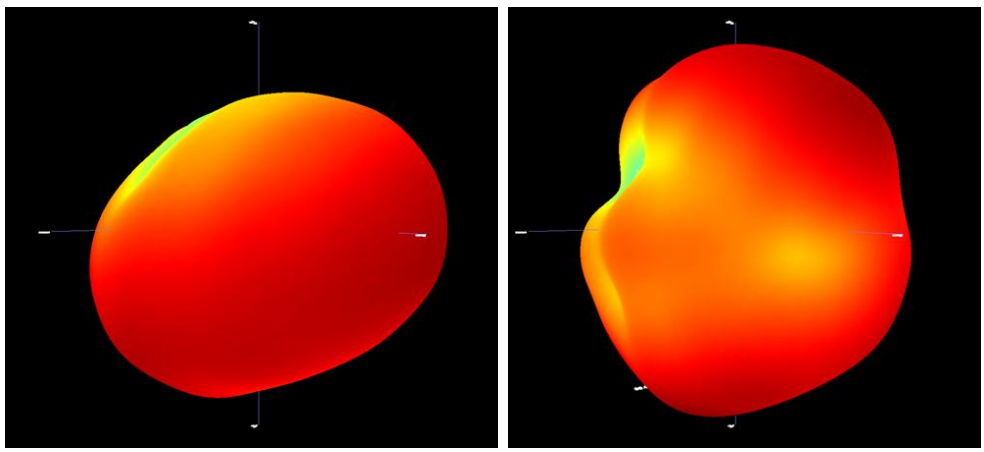

Figure 63. C-Fed Measured Radiation Pattern at 850 MHz (Left) and 1950 MHz (Right)

5.3.5 Correlation

The simulation results show extremely good values for correlation for both the mirrored and duplicated designs. The values are well below the maximum of 0.5 even at the lowest frequencies, as shown in Figure 64. The measured values are not as optimistic, but are still around the 0.5 limit from around 760 MHz and higher.

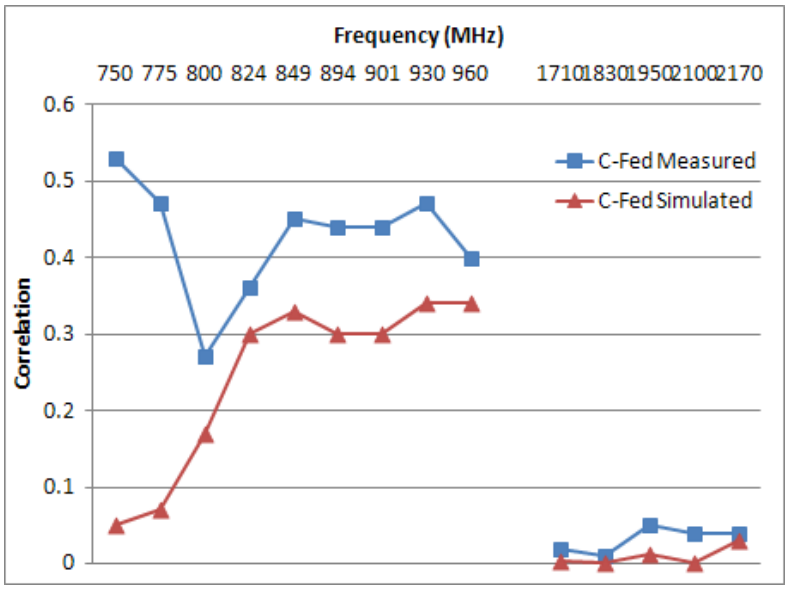

Figure 64. C-Fed Simulated Correlation Coefficient

A comparison of the efficiency and correlation between the mirrored and duplicated designs confirmed the simulation results; that is the mirrored results were typically better. The results are listed in Table 8 below.

TABLE 8. MIRRORED AND DUPLICATED COMPARISON

Frequency (MHz)	Mirrored Efficiency(dB)	Duplicated Efficiency(dB)	Mirrored Correlation Coefficient	Duplicated Correlation Coefficient
750	-5.8	-6.4	0.53	0.55
780	-3.7	-3.6	0.3	0.48
800	-3.3	-2.6	0.27	0.52
820	-4	-3.8	0.37	0.52
850	-3.3	-2.8	0.45	0.52
870	-4.3	-3.7	0.41	0.52
900	-1.8	-2.4	0.45	0.46
930	-2.9	-2.9	0.47	0.51
960	-3.3	-2.5	0.4	0.42

5.3.6 Multiplexing Efficiency

The multiplexing efficiency was calculated for both the measured and simulated results. The results are presented in Figure 65.

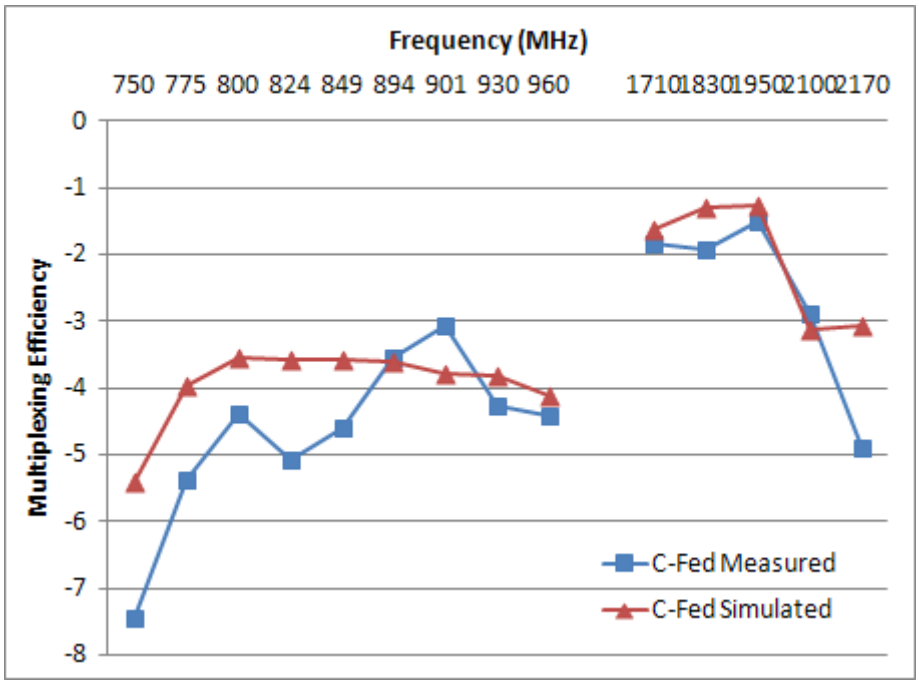

Figure 65. C-Fed Multiplexing Efficiency

5.3.7 SAR

Preliminary SAR simulations were completed for each antenna element across a range of frequencies. An example is given in Figure 66.

The full results are presented in Table 9 below.

TABLE 9. C-FED SAR RESULTS

Frequency (MHz)	780	950	1710	2170
Port 1 SAR (W / kg)	0.4	0.56	0.53	0.226
Port 2 SAR (W / kg)	0.53	0.7	0.82	0.36

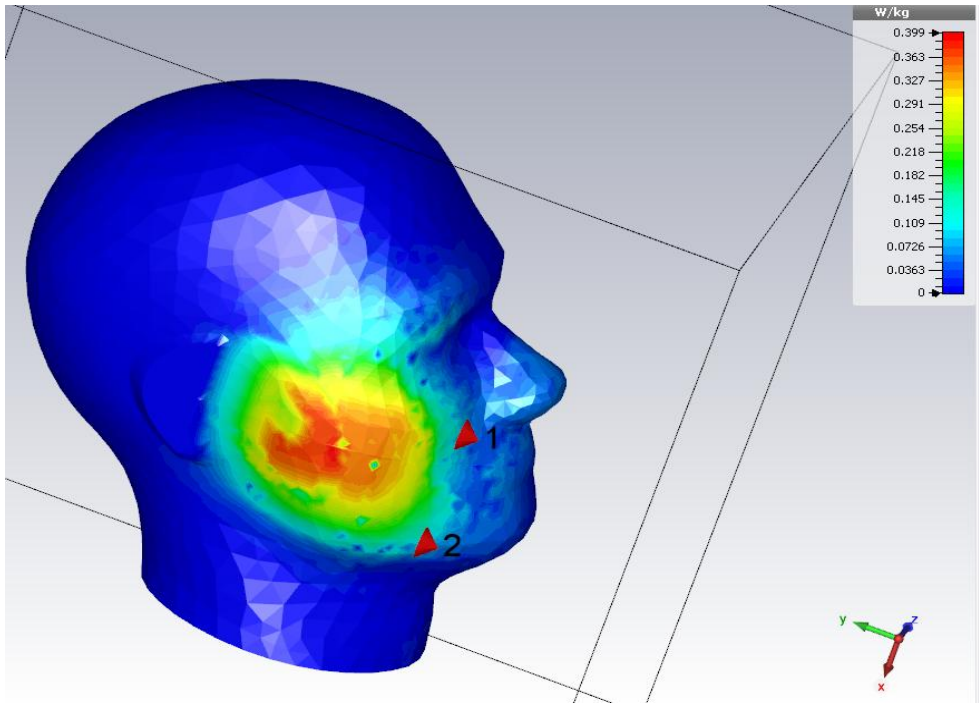

Figure 66. C-Fed 780 MHz SAR Measurement

5.3.8 Battery Effects

A battery was added in the same manner as the other two designs and the effect on antenna efficiencies was studied. The results are presented in Figure 67.

Introducing the battery, even at the edge of the board results in almost no drop in efficiency except for at very high frequencies.

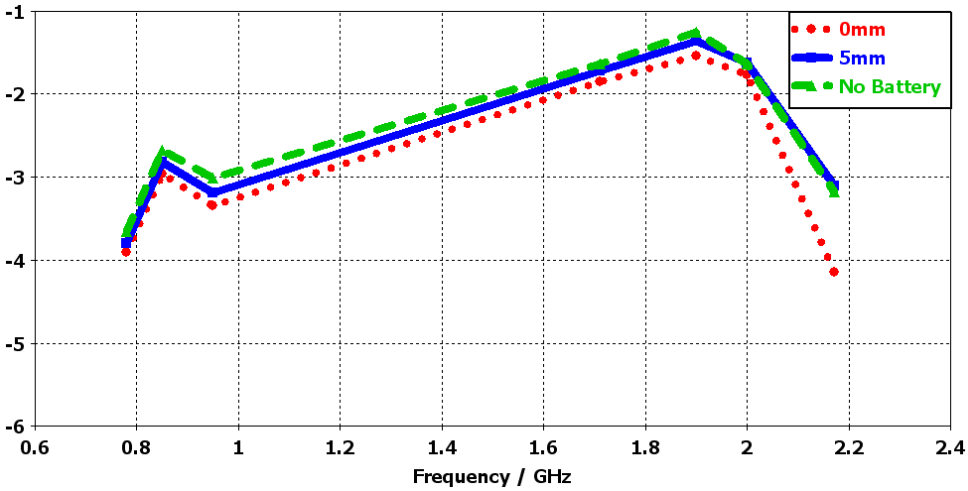

Figure 67. C-Fed Battery Effects

5.4 Conclusions

This design shows great promise for fulfilling all the requirements. Overall, the performance is quite close to that of the reference design, and the main limitation seems to be the isolation between the elements, but if other system tradeoffs are acceptable, or if the design can be further optimized, it may be possible to implement this configuration in a real phone.

CHAPTER 6

6 Summary of Results and Comparisons

6.1 Total Size Comparison

In the mobile phone development process, the total volume occupied is tightly restricted and space efficiency is critical. Therefore a comparison is done below to show the differences in size between three designs presented in this thesis.

TABLE 10. VOLUME COMPARISON

Design	Width (mm)	Height (mm)	Depth (mm)	Volume $(mm)^3$
Reference	60	12	7	5040
L-Fed	66	10	10	6600
C-Fed	66	10	5	3300

The C-Fed design occupies the smallest total volume, while the Reference design has the smallest width. The L-Fed design is large in every dimension and unfortunately covers a smaller bandwidth.

6.2 Efficiencies and Bandwidths

Comparisons between the designs for both simulated and measured data are analyzed in this chapter. The first comparison is between the return losses of the three designs. Figure 68 shows the simulated reflection coefficients, and Figure 69 shows the measured values from the prototypes.

The C-Fed and Reference designs clearly show superior bandwidth potential, although the L-Fed design provides the cleanest and easiest response to understand.

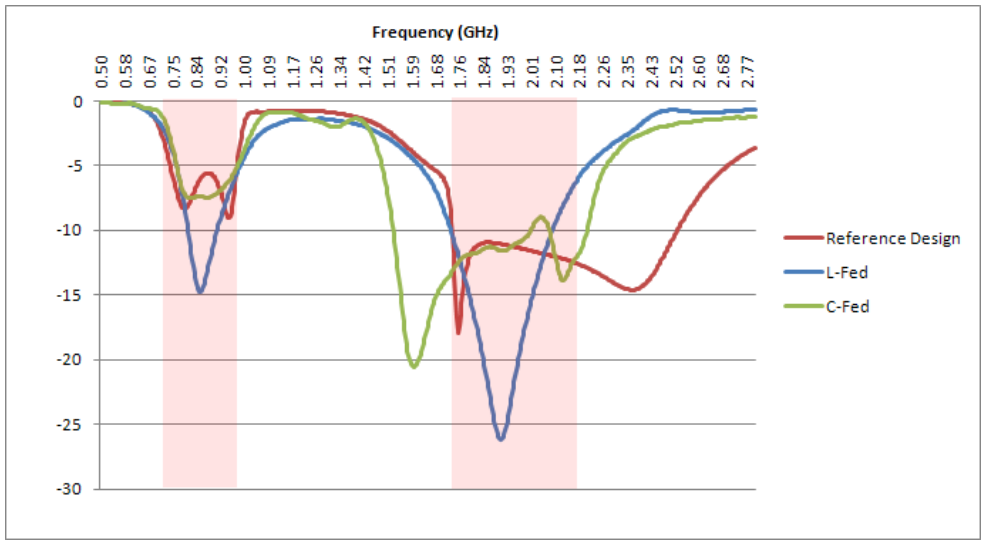

Figure 68. Simulated Reflection Coefficient Comparison

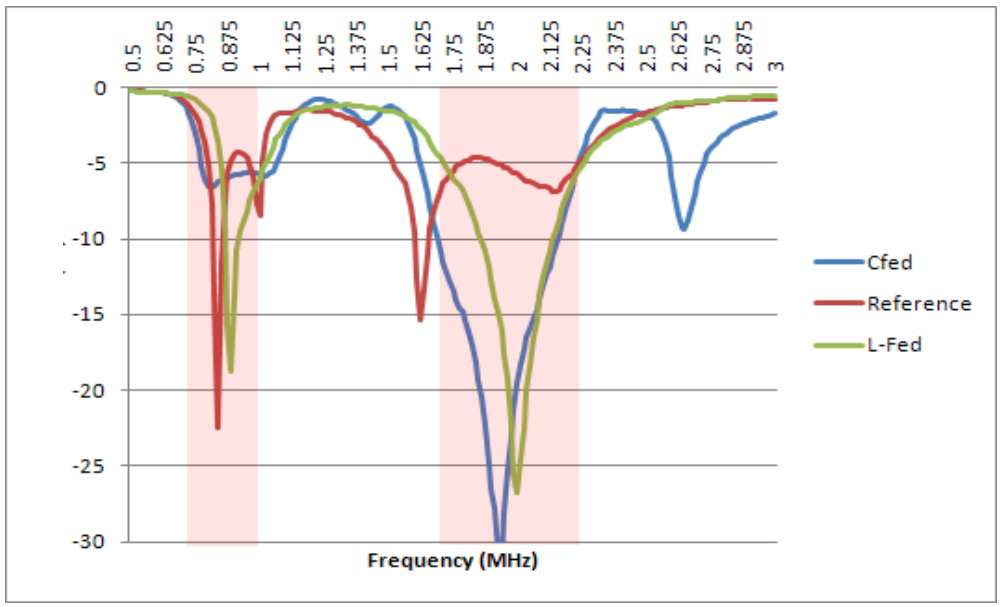

Figure 69. Measured Reflection Coefficient Comparison

The measured results follow the simulated results quite closely, though the C-Fed is the clear winner in this category.

The simulated and measured efficiencies are compared in Figure 70.

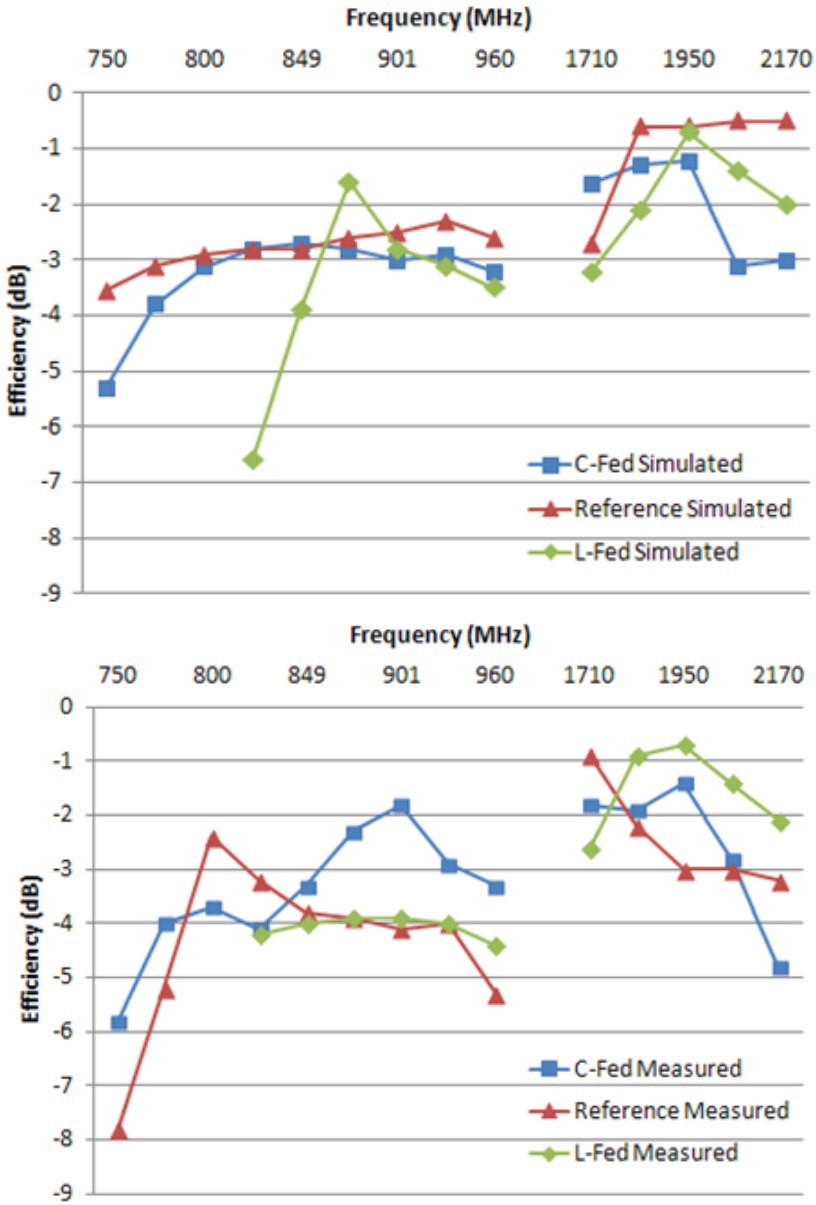

Figure 70. Simulated (Upper) and Measured (Lower) Efficiency Comparison

The bandwidth limitation of the L-Fed is again clear in the efficiency comparison, with the other two designs showing similar results.

6.3 Isolation

The simulated and measured isolation performance of the three designs are shown in Figure 71 and Figure 72, respectively. The L-Fed design clearly performs the best in this regard, with the other two designs having a similar minimum isolation of around 7 dB. The C-Fed design has the poorest isolation across both the highband and lowband. The simulated and measured results agree well with each other.

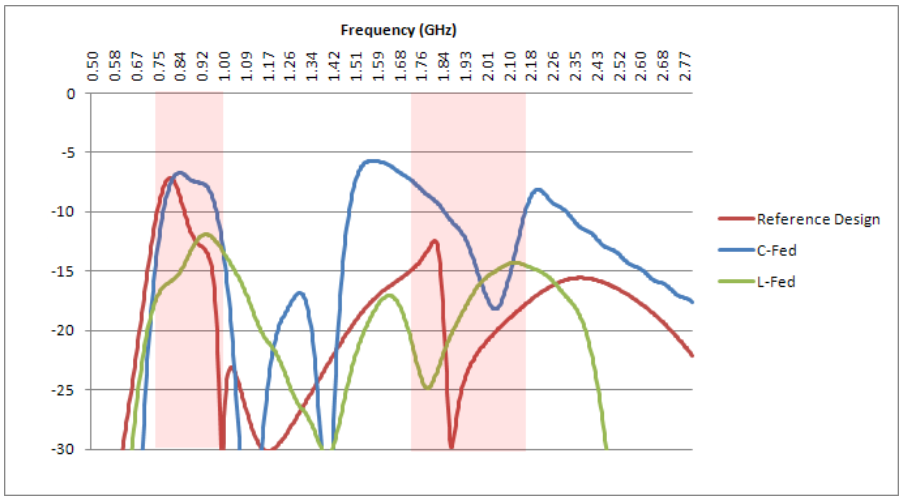

Figure 71. Simulated Coupling Coefficient Comparison

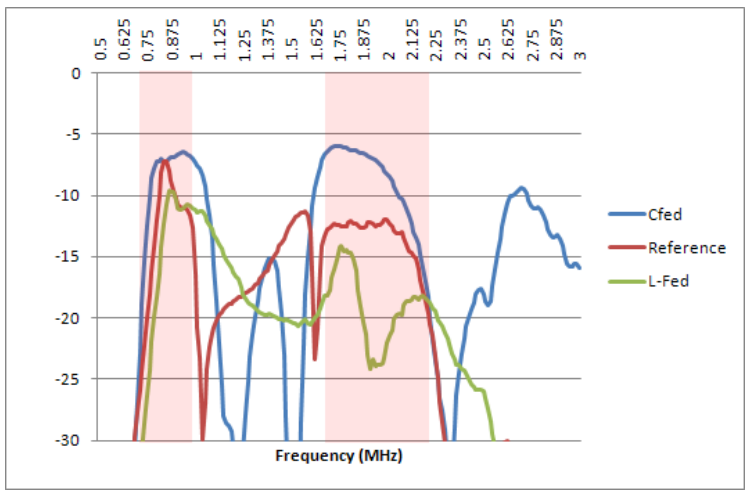

Figure 72. Measured Coupling Coefficient Comparison

6.4 Correlation

A comparison of the correlation between the three designs for both measured and simulated results are shown in Figure 73. All the designs are well within specification for the highband, but the C-Fed is the closest to passing the specification in the lowband.

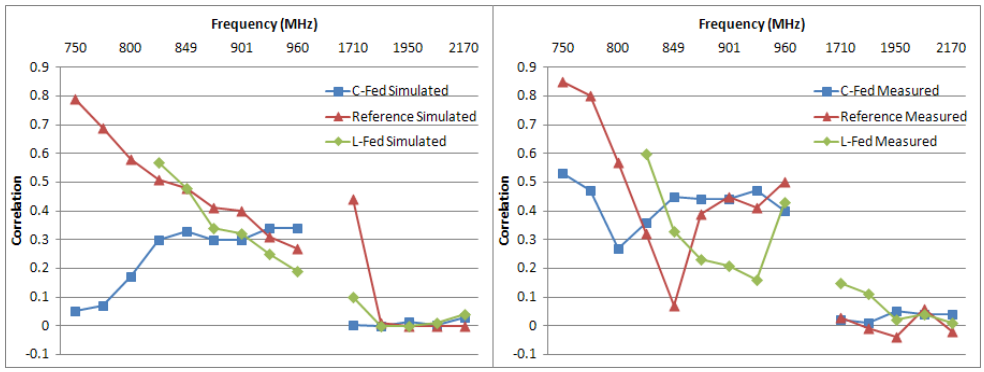

Figure 73. Simulated (Left) and Measured (Right) Correlation Comparison

6.5 Multiplexing Efficiency

Finally, the multiplexing efficiency is compared in Figure 74. The performance of all three designs is quite similar, with the L-Fed performing comparably in the limited frequency range that it spans in the lowband.

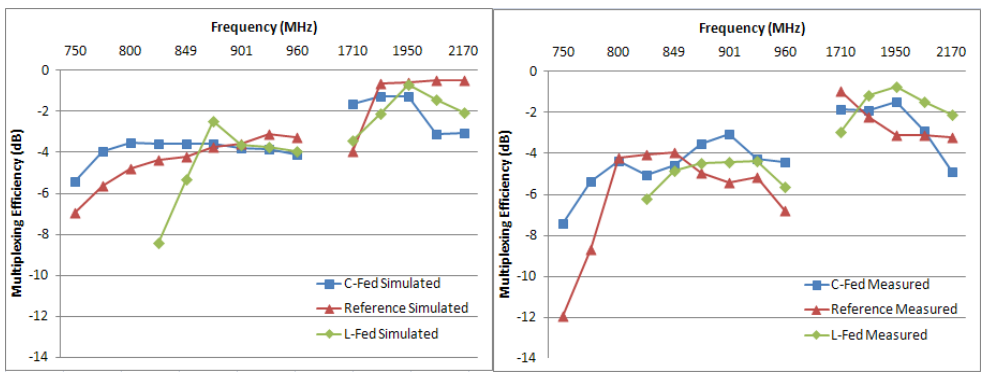

Figure 74. Simulated (Left) and Measured (Right) Multiplexing Efficiency Comparison

CHAPTER 7

7 Conclusions

7.1 Analysis of the Designs

The results of the previous chapter show that each design has its own merits, and as with all antenna design, the selection will be very application-dependent.

For the scope of this project, covering the frequency bands of Table 1 in a full-duplex manner, the C-Fed and reference designs are the most promising and show near-equal performance with a similar amount of space allocated. The C-Fed design shows promise for achieving the performance in a smaller volume, but the reference design achieves the same isolation values with the antenna elements located physically closer.

The selection may ultimately come down to other factors such as SAR performance, ease of design/fabrication, and response to hand and battery effects.

The L-Fed design may be an ideal alternative when MIMO operation is not required and only one antenna is selected at any time to reduce hand or body effects [5]. However, future devices using this technology will likely need to employ structures with higher bandwidth potential.

7.2 Suggestions for Future Work

Although the design variants were explored in a great deal of detail, the results suggest the following areas of study may provide further insight.

1) Moving the two new designs from the mock-up phase to a more realistic implementation will bring about its own set of challenges with having the parts machined and understanding the effect that the

geometry change will have. Some of the practicalities that could come with this might include a more rigorous study of hand effects and SAR performance.

2) It may prove beneficial to add active switching to extend the bandwidths, particularly when it comes to the lower block of 700 MHz frequencies, the addition of switching could provide the additional margin necessary for each design variant to be viable for use in a production model.

3) More advanced matching networks between the various feeds and antennas did not prove to be wholly effective in previous work on a monopole structure [21], but may be worth studying in more detail on these or similar designs.

References

[1] http://en.wikipedia.org/wiki/File:DynaTAC8000X.jpg.

[2] http://en.wikipedia.org/wiki/File:VX8300.JPG.

[3] http://en.wikipedia.org/wiki/File:NTT_DOCOMO_XPERIA_ACRO_SO-02C_Front.JPG.

[4] M. Jensen and Y. Rahmat-Samii, "EM Interaction of Handset Antennas and a Human in Personal Communications," *Proceedings of the IEEE*, pp. Vol. 83, No. 1, 1995.

[5] S. Zhang, Z. Ying, and S. He, "Compact Adaptive Wideband LTE MIMO Antenna Array with Four Elements for Mobile Terminals," in *International Workshop on Antenna Technology*, Tucson, AZ, USA, 2012.

[6] B. K. Lau, "Multiple Antenna Terminals," in *MIMO: From Theory to Implementation*. San Diego: Academic Press, 2011, pp. 267-297, ISBN: 978-0-12-382194-2.

[7] V. Plicanic, "Antenna Diversity Studies and Evaluation," Lund, Master of Science Thesis 2004.

[8] A. Paulraj, R. Nabar, and D. Gore, *Introduction to Space-Time Wireless Communications*. New York: Cambridge University Press, 2003, vol. ISBN: 978-0-521-06593-1.

[9] M. B. Knudsen and G. F. Pedersen, "Spherical Outdoor to Indoor Power Spectrum Model at the Mobile Terminal," *IEEE Sel. Areas Commun.*, pp. Vol. 20, No. 6, pp 1156-1168, 2002.

[10] R. Tian, B. K. Lau, and Z. Ying, "Multiplexing Efficiency of MIMO Antennas," *IEEE Antennas Wireless Propagation Letters*, pp. Vol. 10 pp. 183-186, 2011.

[11] 3D EM Field Simulation - Computer Simulation Technology. [Online]. http://www.cst.com/

[12] K. Yee, "Numerical Solution of Initial Boundary Value Problems Involving Maxwell's Equations in Isotropic Media," *IEEE Transactions on Antennas and Propagation*, pp. Vol. 14 Issue 3 pp 302-307, 1966.

[13] A. Taflove, "Application of the Finite-Difference Time Domain Method to Sinusoidal Steady-State Electromagnetic Penetration Problems," *IEEE Transactions on Electromagnetic Compatibility*, pp. Vol. EMC-22 No. 3, 1980.

[14] BetaMatch. [Online]. http://www.mnw-scan.com/index.html

[15] K. Rosengren, P. Kildal, C. Carlsson, and J. Carlsson, "Characterization of Antennas for Mobile and Wireless Terminals by Using Reverberation Chambers: Improved Accuracy by Platform Stirring," in *IEEE Antennas and Propagation International Symposium*, 2001.

[16] A. A. H. Azremi, H. G. Shiraz, and P. S. Hall, "Small Antenna Efficiency by the Reverberation Chamber and the Wheeler Cap Methods," in *IEEE 7th Malaysia International Conference on Communication*, 2005, pp. Vol. 1 pp 12-16.

[17] Z. Lin, "Channel Sounding in Reverberation Chamber - Calibration for Measurements of Wireless Devices," Gothenburg, Sweden, Master of Science Thesis Project 2009.

[18] K. L. Wong and C. T. Lee, "Wideband Surface-Mount Chip Antenna for Eight-Band LTE/WWAN Slim Mobile Phone Application," *Microwave and Optical Technology Letters*, pp. Vol. 52, No. 11, 2010.

[19] X. Xu and Y. E. Wang, "Chu's Limit and Switched Electrically Small Antennas," in *IWAT '07: Antenna Technology: Small and Smart Antennas Metamaterials and Applications*, 2007.

[20] K. L. Wong, *Compact Broadband Microstrip Antennas*. New York: John Wiley & Sons, Inc., 2002.

[21] M. Håkansson, "Decoupling Techniques for a Multi-band Antenna System," Lund, Master of Science Thesis 2010.

[22] W. Geyi, Q. Rao, S. Ali, and D. Wang, "Handset Antenna Design: Practice and Theory," vol. Prog Electromagn. Res., no. Vol. PIER 80, pp 123-160.

[23] Q. Rao, S. Ali, and D. Wang, "Compact 3-D monopole antenna for," U.S. Patent Appl. 33246.

[24] Q. Rao and K. Wilson, "Design, Modeling, and Evaluation of a Multiband MIMO/Diversity Antenna System for Small Wireless Mobile Terminals," vol. vol.1, issue 3, pp 410-419, 2011.

[25] Y. Rahmat-Samii M. Jensen, "EM Interaction of Handset Antennas and a Human in Personal Communications," p. Vol. 81 No. 1, 1995.

[26] J. Kraus and R. Marhefka, *Antennas for All Applications*. New York: Tata McGraw-Hill Publishing Company Limited, 2001, vol. 0072321032.

[27] E. Newman and C. H. Walter, "Two Methods for the Measurement of Antenna Efficiency," *IEEE Transactions on Antennas and*

Propagation, pp. Vol. AP-23 No. 4, 1975.

[28] V. Plicanic, B. K. Lau, and Z. Ying, "EM Interaction of Handset Antennas and a Human in Personal Communications," in *International Workshop on Antenna Technology: Small Antennas and Novel Metamaterials*, 2008.

[29] ICNIRP, "Guidelines for Limiting Exposure to Time-Varying Electric, Magnetic, and Electromagnetic Fields," *Health Physics*, pp. Vol. 74, pp 494-522, 1998.